LA-UR-21-21187
Approved for public release; distribution is unlimited.

Title:	Photoinjectors, Emittance Revisited, Photoinjector Design & Optimization
Author(s):	Nguyen, Dinh C. Anisimov, Petr Mikhaylovich Neveu, Nicole
Intended for:	USPAS 21 lecture slides
Issued:	2021-02-09

U.S. Particle Accelerator School
January 25 – February 19, 2021

VUV and X-ray Free-Electron Lasers

Photoinjectors, Emittance Revisited, Photoinjector Design & Optimization

Dinh C. Nguyen,[1] Petr Anisimov,[2] Nicole Neveu[1]

[1] SLAC National Accelerator Laboratory

[2] Los Alamos National Laboratory

U.S. DEPARTMENT OF ENERGY | Stanford University

SLAC NATIONAL ACCELERATOR LABORATORY

Los Alamos NATIONAL LABORATORY EST. 1943

Wednesday (February 3) Lecture Outline

	Time
• Introduction to Photoinjectors	10:00 – 10:30
• Emittance Revisited	10:30 – 11:00
• Break	11:00 – 11:05
• Photoinjector Designs	11:05 – 11:30
• Optimization & Beam Shaping (by Nicole Neveu)	11:30 – 12 Noon

Introduction to Photoinjectors

Photoinjector System

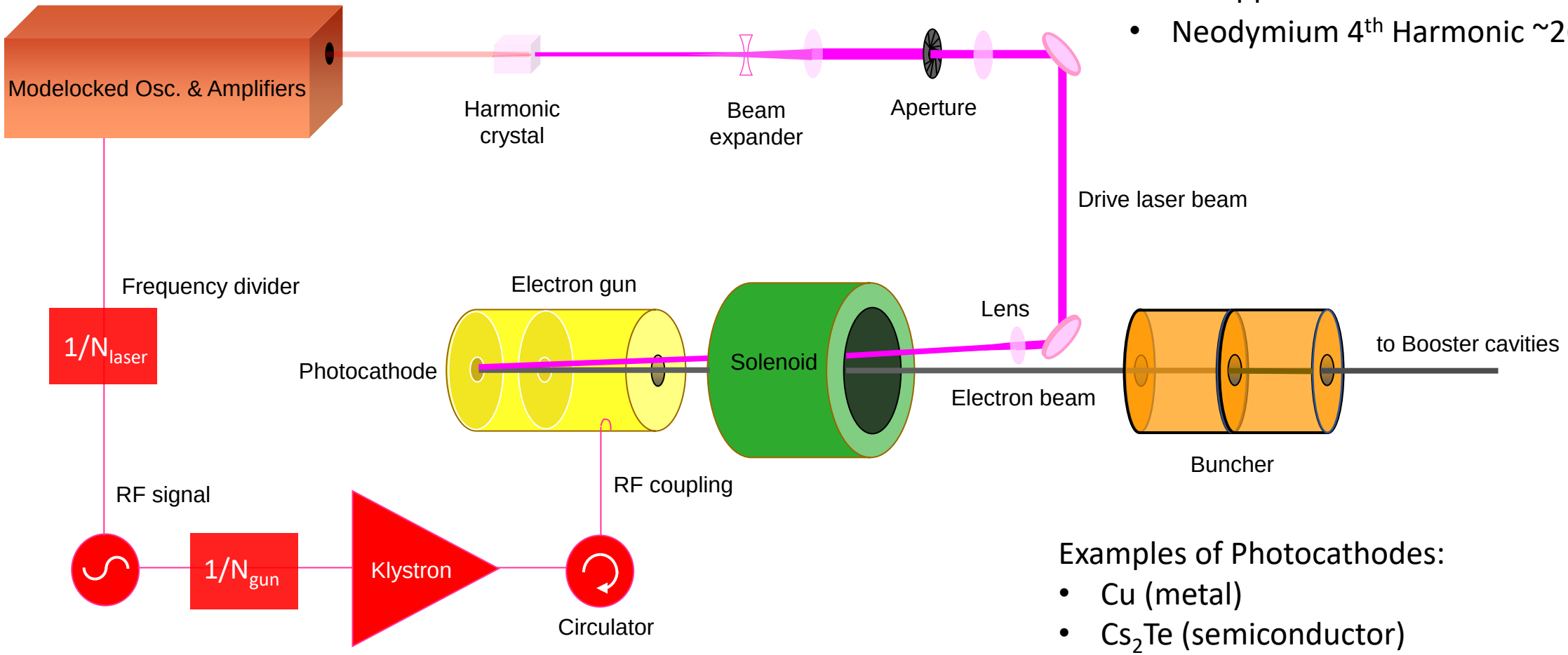

Examples of Drive Lasers

- Ti:Sapphire 3rd Harmonic ~260 nm
- Neodymium 4th Harmonic ~266 nm

Examples of Photocathodes:

- Cu (metal)
- Cs_2Te (semiconductor)

Components of a Photoinjector

A photoinjector has the following major components:

- an **ELECTRON GUN** that accelerates electrons to kinetic energy of a few MeV or less,
- a **PHOTOCATHODE** that produces picosecond electron bunches when gated with UV or visible laser pulses at photon energy above the photocathode bandgap or work function,
- a **DRIVE LASER** to gate the photoemission of electrons from the photocathode,
- a **SOLENOID MAGNET** to perform emittance compensation (sometimes, there is also a BUCKING COIL to zero out the magnetic field at the photocathode),
- **BUNCHER/BOOSTER** cavities to compress and accelerate the electron bunches to sufficiently high energy in order to mitigate the effects of space charge.

In this lecture, we discuss the generation of high-brightness beams in a photoinjector, an RF electron gun with laser gated photoemission. We revisit the concept of emittance and brightness. We analyze the processes that lead to emittance growth in the photoinjector and the emittance compensation technique. Finally, we review different designs of photoinjectors to produce the high-brightness electron beams to drive the x-ray FEL.

Schematic of an RF photoinjector

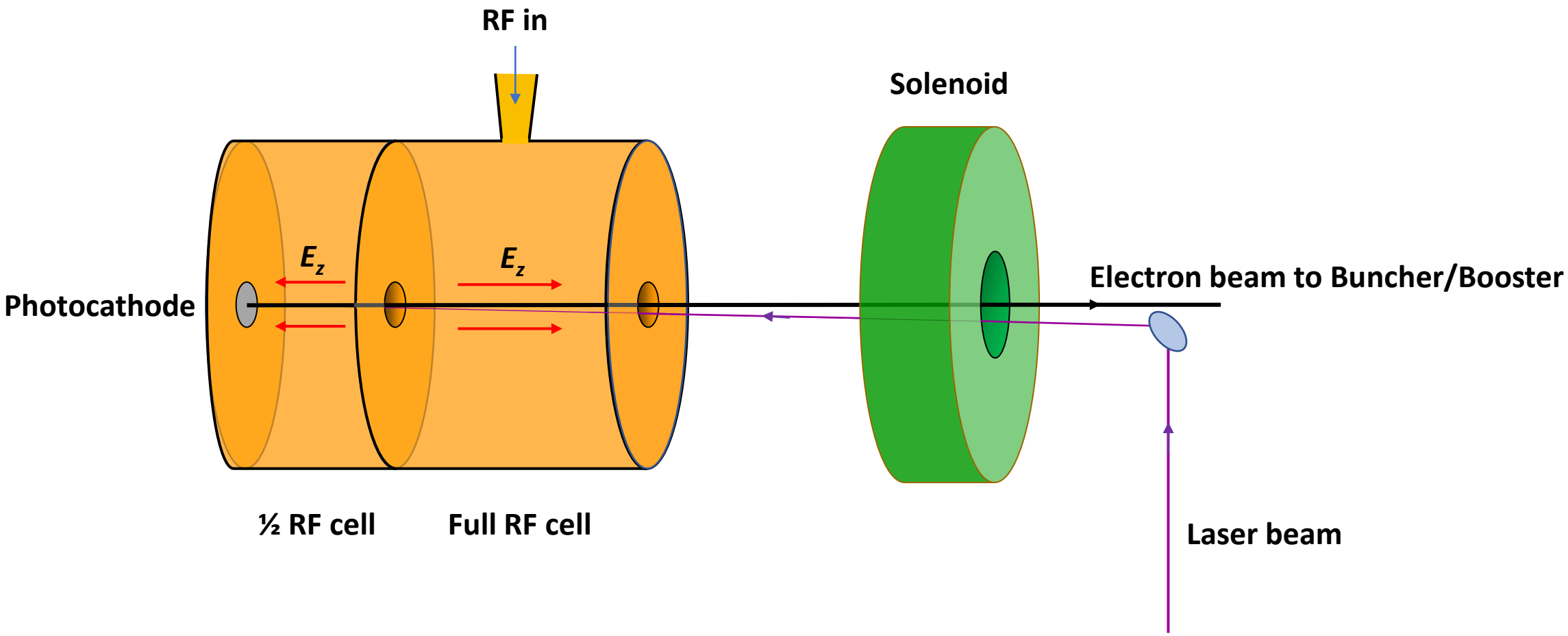

(n + 1/2)-Cell Photoinjector

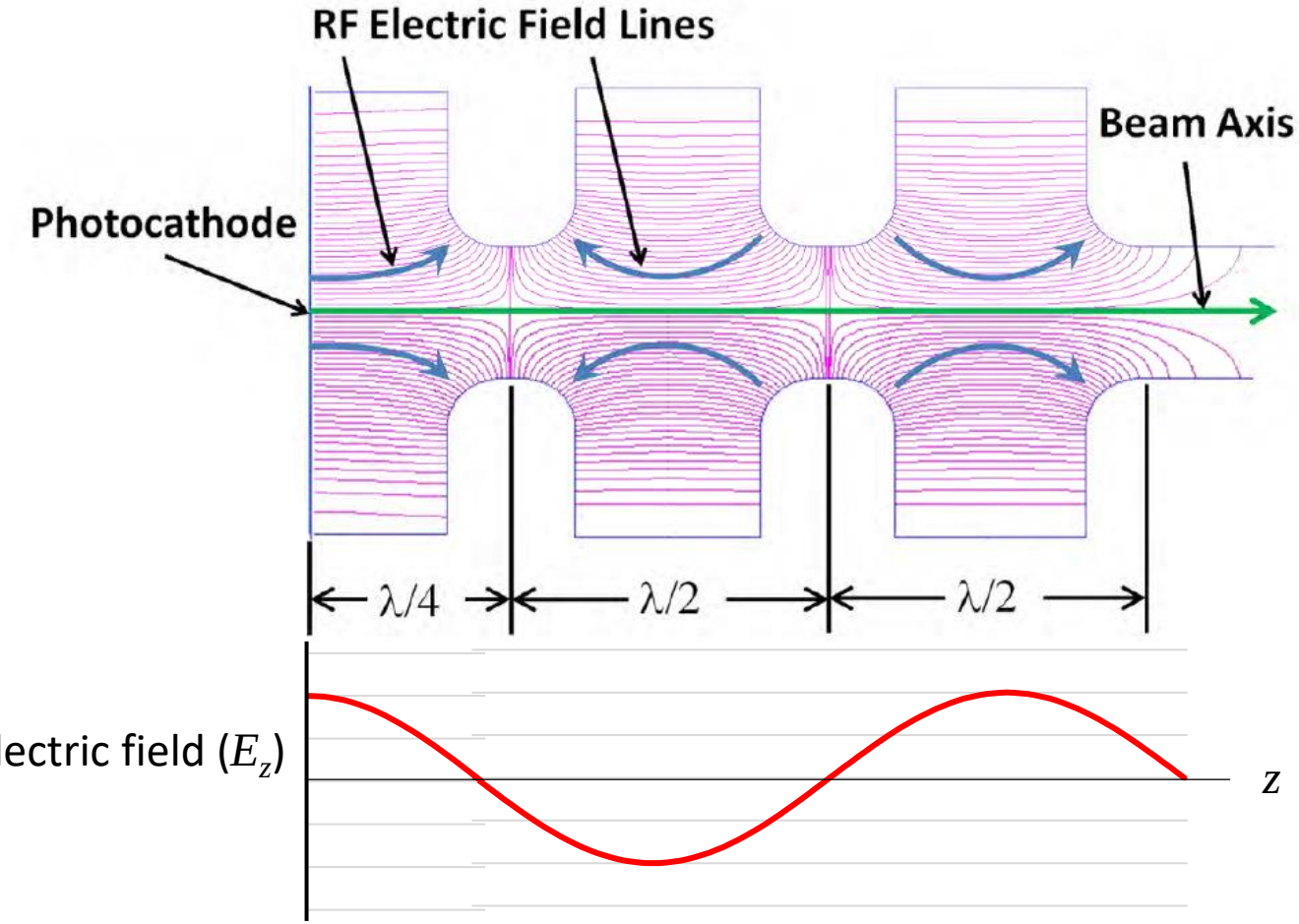

The RF photoinjector was invented by Fraser and Sheffield at LANL as a high-brightness electron source for FEL.
J.S. Fraser, R.L. Sheffield and E. Gray, *Nucl. Instr. Meth.* A 250 (1986) pp. 71-76.

Photoemission versus Thermionic Emission

Photoemission

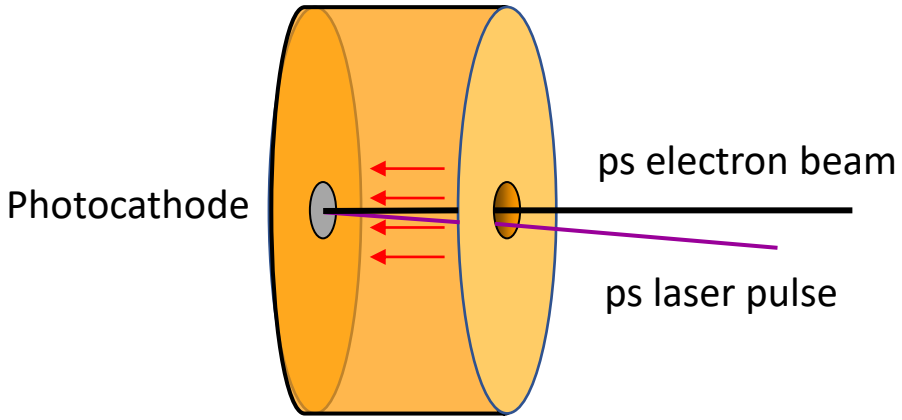

- Electrons are generated by ps laser pulses
- High current density, typically >200 A/cm^2
- High electron brightness in 6D phase space
  - ➢ High peak current
  - ➢ Small transverse emittance
  - ➢ Brightness ~ 10^{15} A/(m-rad)^2

Thermionic Emission

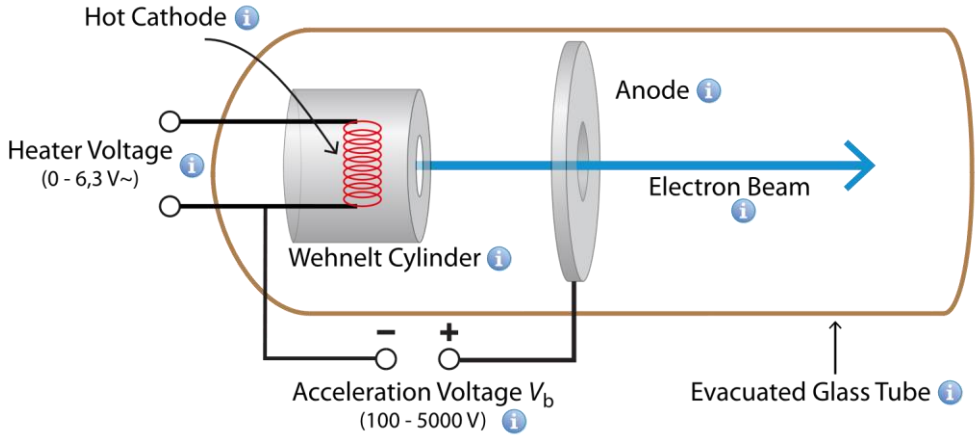

- Electrons are “boiled off” from a hot cathode
- Low current density, typically <10 A/cm^2
- Long electron pulses requiring bunch compression
  - ➢ Particle loss in bunch compression
  - ➢ Emittance growth
  - ➢ Brightness < 8 x 10^8 A/(m-rad)^2

Three-step Photoemission Process

p-type Semiconductor

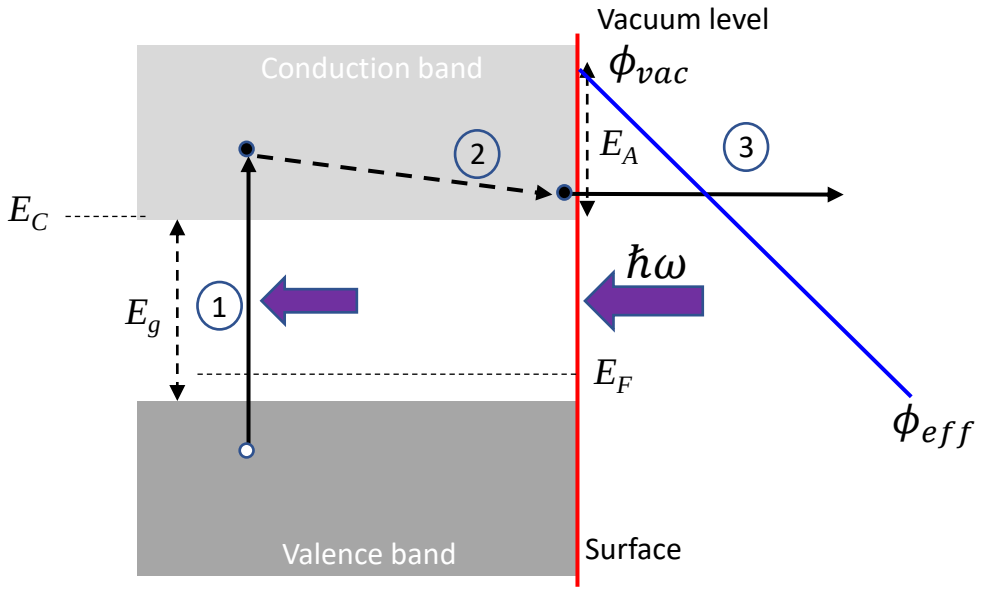

Electron affinity $E_A = \phi_{vac} - E_C$

Effective vacuum level $\phi_{eff} = \phi_{vac} - E_0 z$

Photon energy and bandgap energy $\hbar\omega > E_g$

1. Photo-excitation
   - Reflection loss at the photocathode surface
   - Attenuation inside material (penetration depth)
   - Excitation of electrons into conduction band
2. Electron transport to surface
   - Electron-electron scattering
   - Electron-phonon scattering
3. Electron escape from surface
   - Barrier tunneling
   - Schottky effect (field enhancement)

Positive electron affinity semiconductor (e.g., Cs_2Te)
Negative electron affinity (e.g., Cs:GaAs).

Photocathode Quantum Efficiency

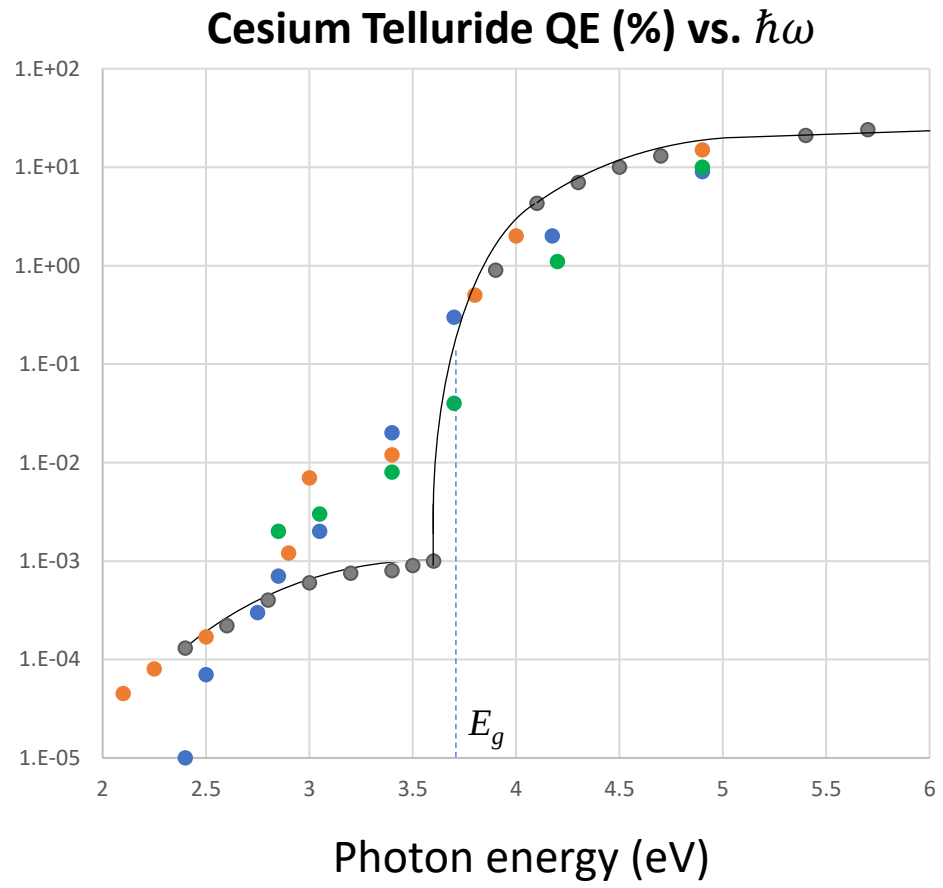

Ce_2Te bandgap = 3.7 eV

Reflectivity

Pulse energy

Bunch charge $q = (1 - R)\frac{W}{\hbar\omega} QE$

Reflectivity depends on angle of incidence and wavelength
QE depends on materials and photon energy

Typical values for Cs_2Te at normal incidence

$q = 160\ pC$

$R = 4\%$

$W = 15\ nJ$

$QE = 5\%$

$\hbar\omega = 4.5\ eV$

Photoemission from a Metal Photocathode

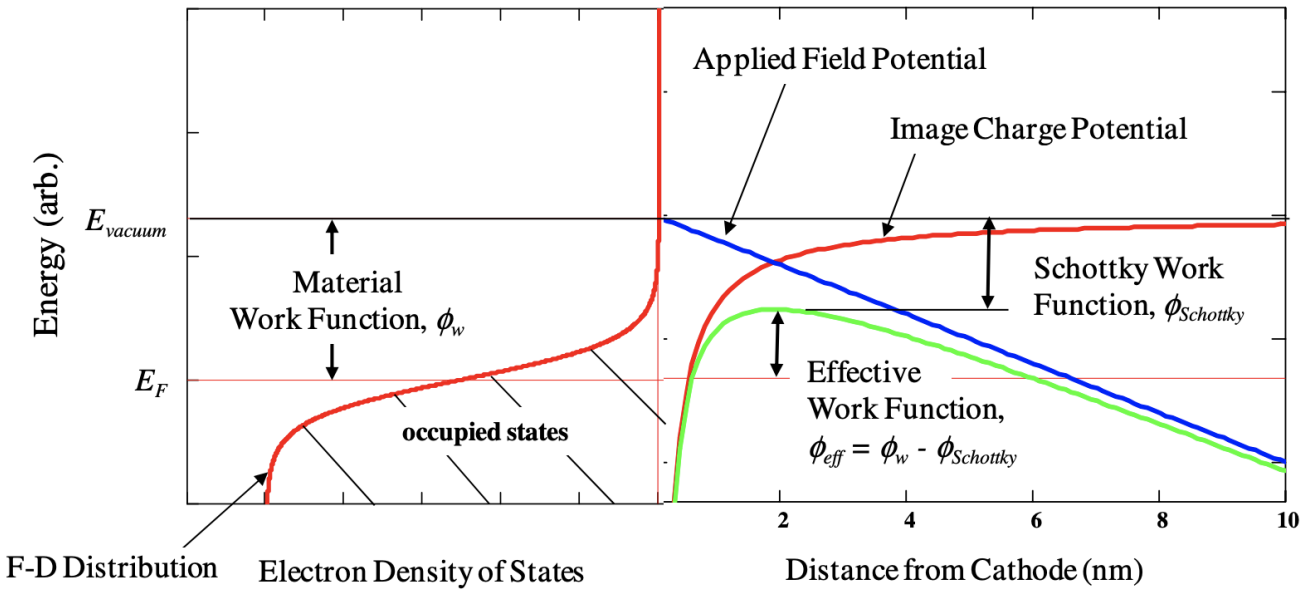

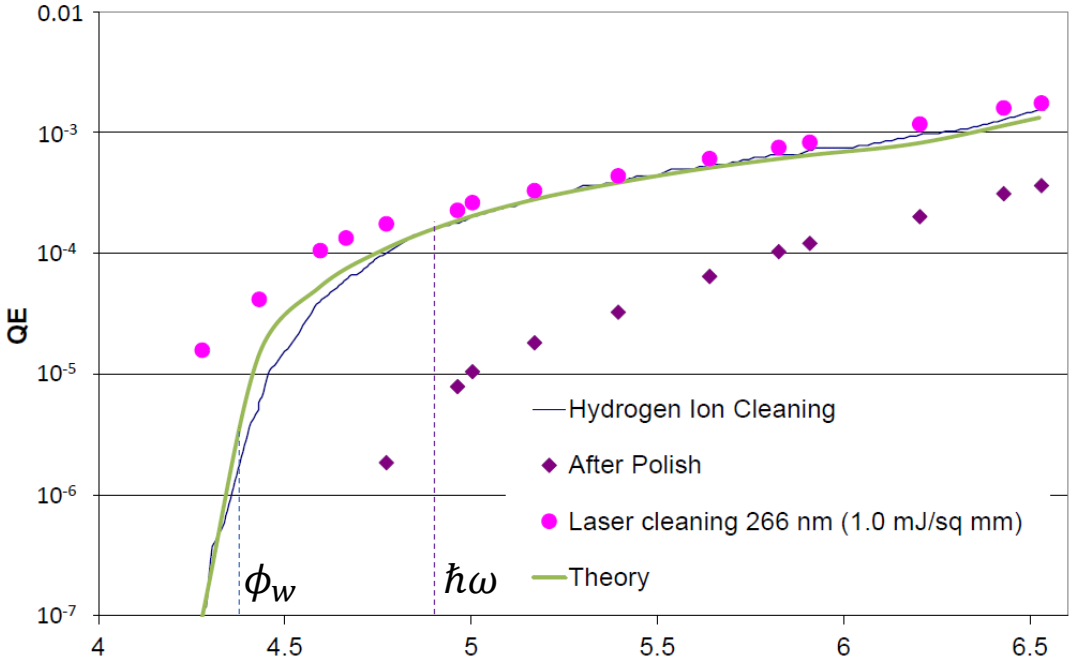

Field-enhanced photoemission

$$QE = a\left[\hbar\omega - \left(\phi_w - \sqrt{\frac{\beta e E_0}{4\pi\epsilon_0}}\right)\right]^2$$

$q = 160\ pC$

$R = 40\%$

$QE = 0.01\%$

$\hbar\omega = 4.9\ eV$

$W = 13\ \mu J$

Copper photocathode requires ~1,000X higher pulse energy compared to Cs_2Te

Image Charge Field

Gauss law: a pancake of electrons with charge q over an area A produces an image electric field opposing the applied electric field at the cathode.

Cathode field $$E_{cathode} = E_{applied} - E_{image}$$

Image charge field $$E_{image} = \frac{q}{\epsilon_0 A}$$

At -60° (30°) injection phase, the applied field is only one-half of the maximum RF field. The smaller applied field at injection and the image charge field set the maximum bunch charge that can be extracted. Due to the image charge field, the slope of photocurrent vs. laser power curve decreases at high laser power (the apparent QE is reduced at high bunch charge).

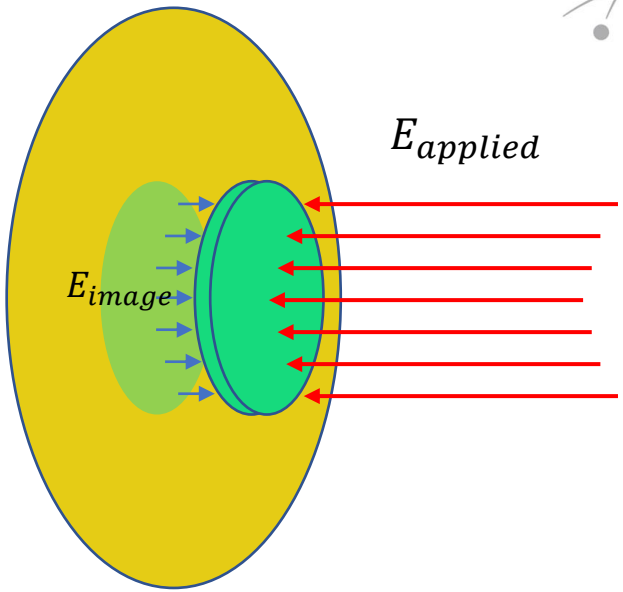

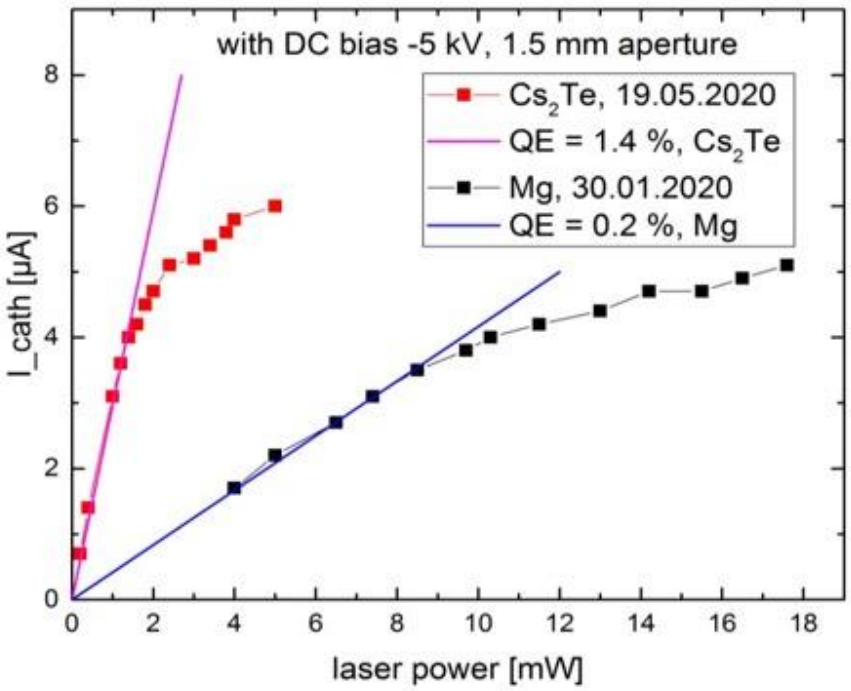

Early Photoinjector Theory

In 1986, Kwang-je Kim developed the early theory for the photoinjector with n + ½ cells based on sinusoidal accelerating field

$$E_z = E_0 \cos(kz) sin(\omega t + \varphi)$$

Since $k = \frac{\omega}{c}$, the accelerating field can be rewritten as

$$E_z = E_0 \cos(kz) sin(kz + \varphi)$$

Near the cathode when the electrons are sub-relativistic, the central particle phase slips behind the RF phase. The phase reaches an asymptotic value as the particles become relativistic.

$$\varphi - \varphi_0 = \omega t - kz$$

$$\varphi - \varphi_0 = \int_0^z \frac{\omega}{v_e} dz - kz = k \int_0^z \frac{c}{v_e} dz - kz$$

1.5-cell photoinjector

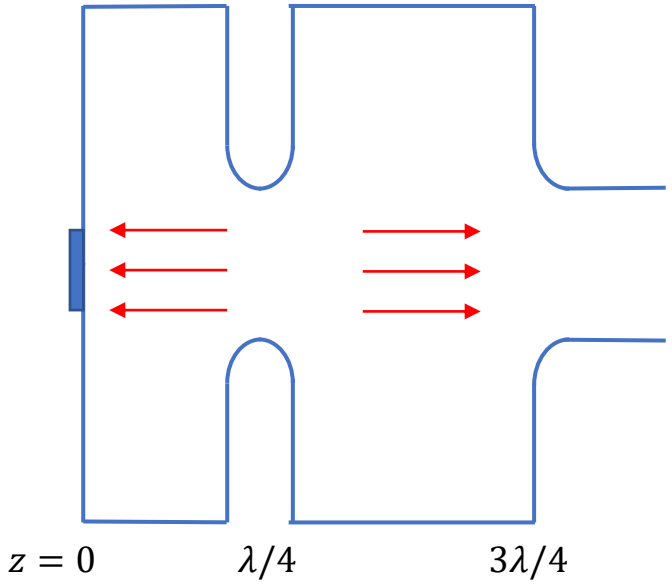

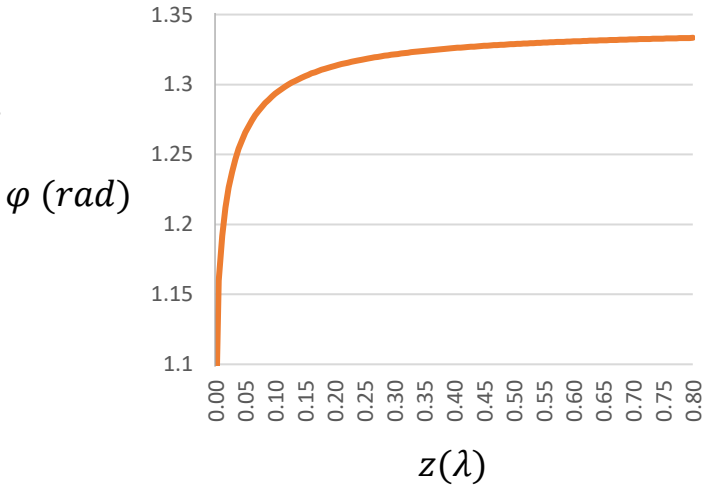

Single Particle Equations of Motion

Lorentz force affecting the particle momentum/energy

$$\frac{d}{dt}(\beta\gamma m_e c) = eE_z$$

$$\frac{d}{dt}(\beta\gamma m_e c) = eE_0 \cos(kz) sin(kz + \varphi)$$

$$\frac{d}{cdt}(\beta\gamma) = \frac{eE_0}{2m_e c^2}\left(\sin(\varphi) + sin(2kz + \varphi)\right)$$

RF phase of the central particle

$$\frac{d\varphi}{dz} = k\left(\frac{1}{\beta} - 1\right)$$

It can be shown that

$$\frac{1}{\beta} = \frac{\gamma}{\sqrt{\gamma^2 - 1}}$$

Change in **particle energy** with respect to z

$$\frac{d\gamma}{dz} = \frac{eE_0}{2m_e c^2}\left(\sin(\varphi) + sin(2kz + \varphi)\right)$$

Change in **particle phase** with respect to z

$$\frac{d\varphi}{dz} = k\left(\frac{\gamma}{\sqrt{\gamma^2 - 1}} - 1\right)$$

These two equations (highlighted) completely describe the evolution of energy and phase of the central particle in a photoinjector, provided that the particle becomes relativistic in the first ½ cell.

Equations of Motion with Scaled Variables

Define the scaled distance $\zeta = kz$

and dimensionless gradient $\alpha = \frac{eE_0}{2km_ec^2}$

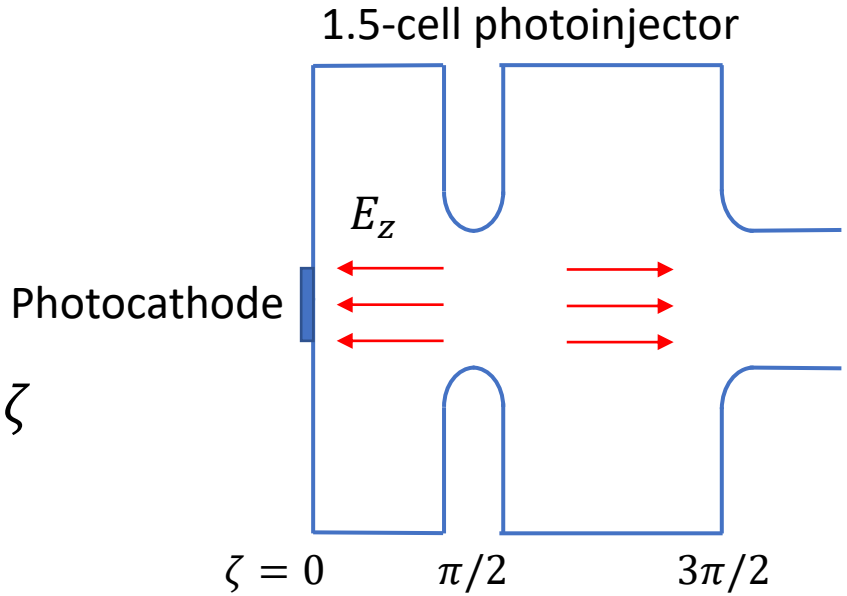

Rates of change in γ and φ with respect to the scaled distance ζ

$$\frac{d\gamma}{d\zeta} = \alpha[\sin\varphi + \sin(\varphi + 2\zeta)]$$

$$\frac{d\varphi}{d\zeta} = \frac{\gamma}{\sqrt{\gamma^2 - 1}} - 1$$

Typical values for the LCLS S-band electron gun

$E_0 = 120\ MV/m$ $\quad m_ec^2 = 0.511MeV$

$k \approx 60\ m^{-1}$ $\quad \alpha \approx 2$

K-J Kim “RF and Space-charge Effects in Laser-driven RF Electron Gun” Nucl. Instr. Meth. A 275, 201-218 (1989).
D. Palmer, PhD thesis “Next Generation Photoinjector” (1998).

Solution to Single-Particle Equation of Motion

Choose an initial solution for γ by ignoring the 2nd term

$$\tilde{\gamma}(\zeta) = 1 + 2\alpha\zeta \sin\varphi_0$$

Plug into the phase equation and integrate

$$\varphi(\zeta) = \frac{1}{2\alpha \sin\varphi_0}\left[\sqrt{\tilde{\gamma}^2 - 1} - (\tilde{\gamma} - 1)\right] + \varphi_0$$

Insert the above into the energy equation and integrate

$$\gamma(\zeta) = 1 + \alpha\left[\zeta \sin\varphi_0 + \frac{1}{2}(\cos\varphi - \cos(\varphi + 2\zeta))\right]$$

Plot of particle energy vs ζ for -60° injection phase

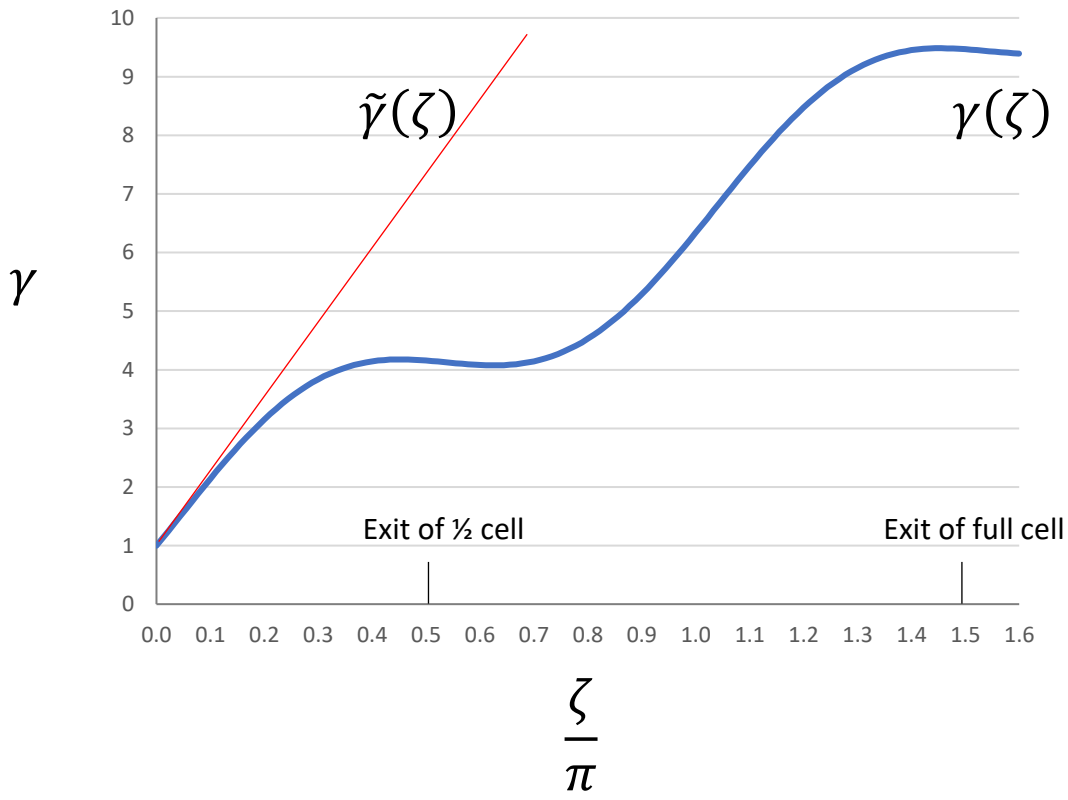

Verify that the electrons are rapidly accelerated to relativistic energy in the first ½ cell, which is one of the assumptions for Kim model to be valid.

Particle Phase at Injection and Exit

Using the convention $E_z(t) = E_0\cos(\omega t + \varphi)$, the injection phase for particles to exit the first cell when $E_z(t) = 0$ is

$$\left(\frac{\pi}{2} - \varphi_0\right)\sin\varphi_0 = \frac{1}{2\alpha}$$

For S-band at E_0 = 120 MV/m, the injection phase should be

$$\varphi_0 = -65^o$$

(25° if using $E_z = E_0\sin(\omega t + \varphi)$)

for electrons to exit the first ½ cell at zero field.

At large γ the particle phase approaches an asymptotic value given by the following equation.

$$\varphi_\infty = \varphi_0 + \frac{1}{2\alpha\sin\left(\varphi_0 + \frac{\pi}{6\sqrt{\alpha}}\right)} + \frac{\pi}{15\alpha}$$

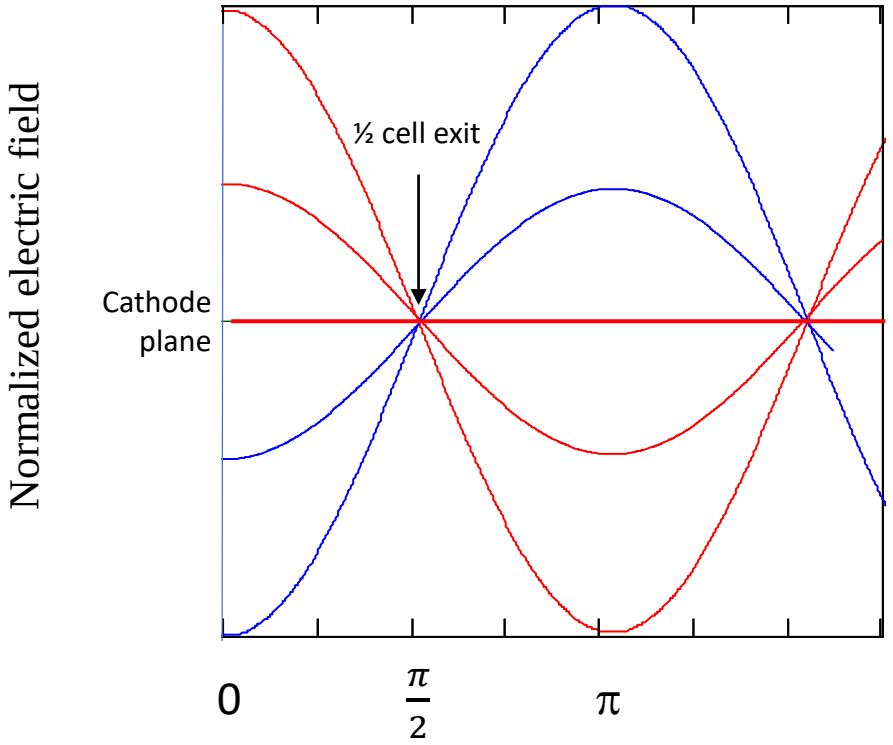

Field when particles are in the first ½ cell

Field when particles are in the second cell

Emittance Revisited

Particle Transverse Positions and Angles

Consider a single electron (red) in an ensemble of billions of particles co-traveling with the reference particle (blue)

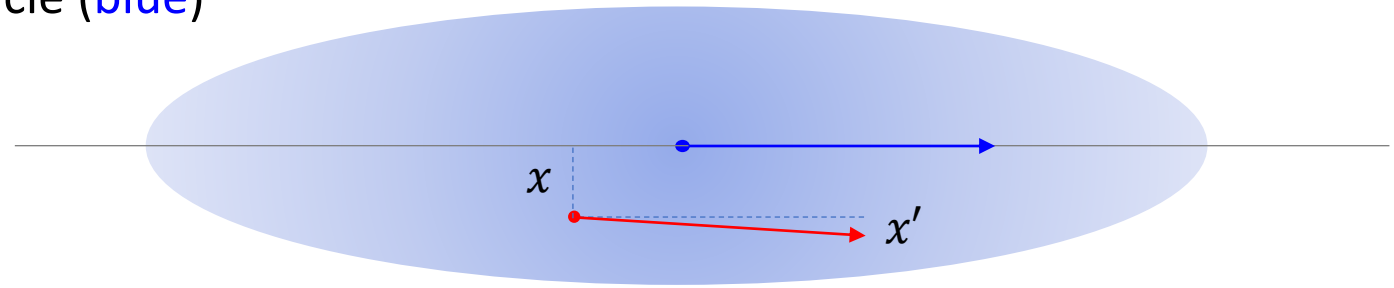

x is the transverse position of the particle with respect to the reference particle

x' is the angle of the particle momentum with respect to the reference particle's momentum

$$x' = \frac{dx}{dz} = \frac{p_x}{p_z} \approx \frac{v_x}{c}$$

Similarly, the particle is also described by its transverse position y and angle y'

Paraxial approximation: transverse velocities are much smaller than c, thus the angles x' and $y' \ll 1$

Laminar Beam (Zero Emittance)

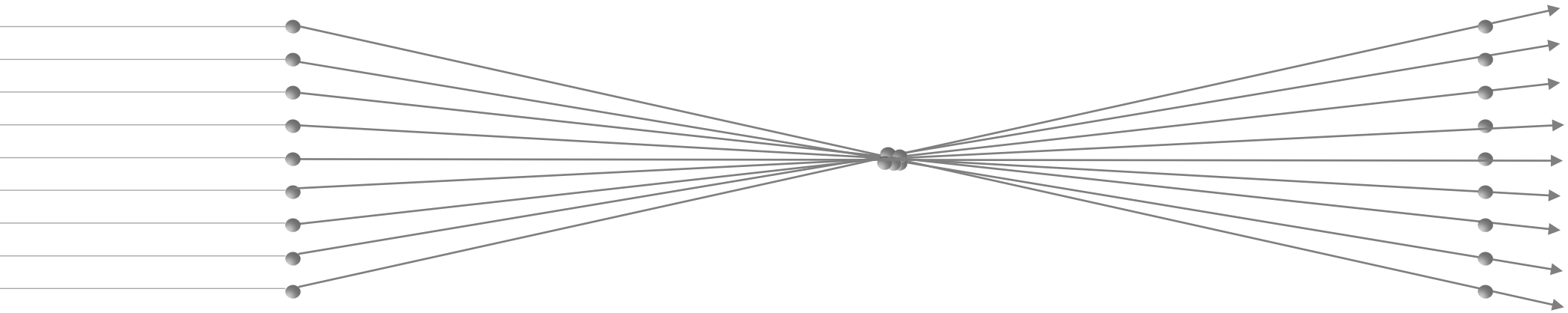

Focusing Lens

Phase space area = 0

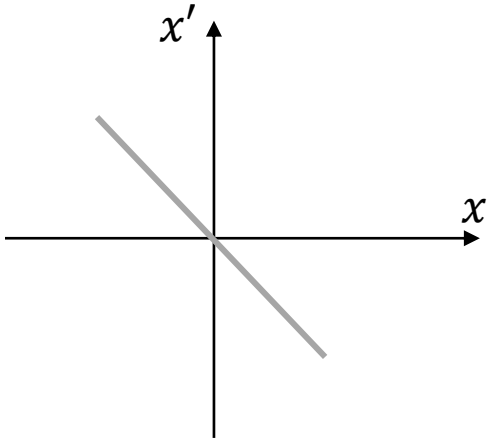

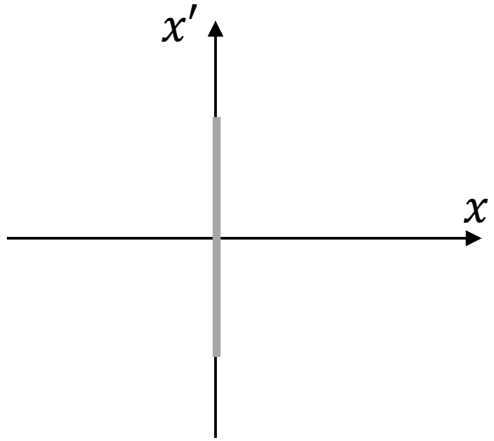

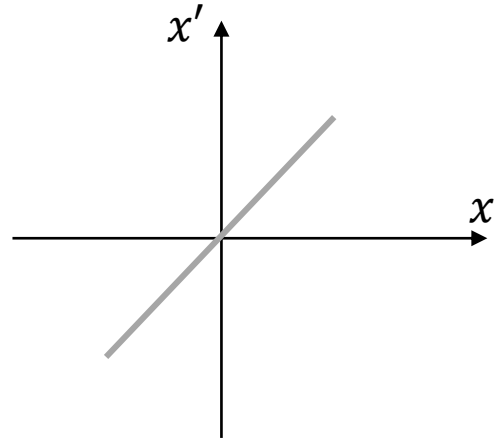

Emittance-dominated Beam

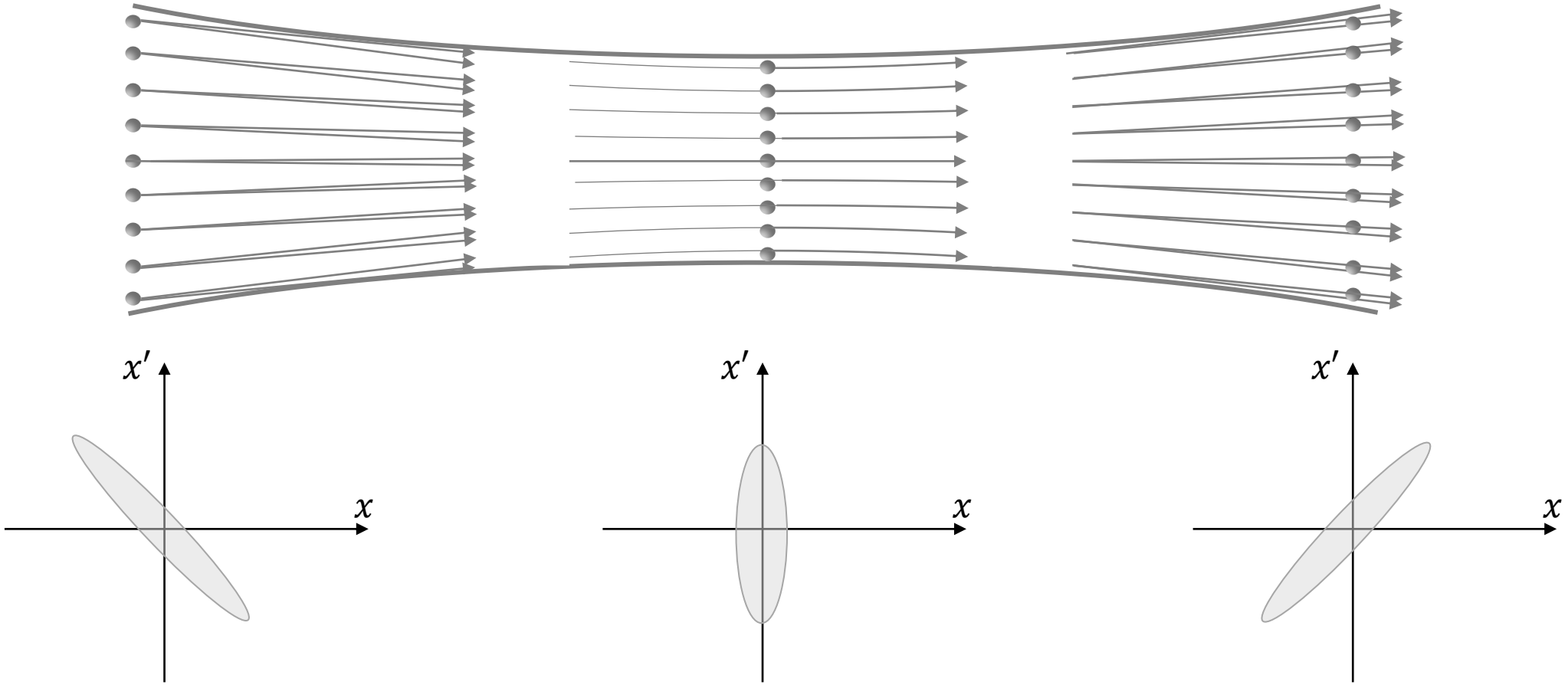

At the beam waist, the ellipse is upright and has a finite phase-space area equal to $\pi\varepsilon_x$

Emittance and Phase-space Area

$$\varepsilon_{x,rms} = \sqrt{\langle x^2 \rangle \langle x'^2 \rangle - \langle xx' \rangle^2}$$

For cases where f is Gaussian distribution in x and x'

$$\langle x^2 \rangle = \frac{1}{2\pi\sigma_x^2} \iint x^2 exp\left(-\frac{x^2}{2\sigma_x^2}\right) exp\left(-\frac{x'^2}{2\sigma_{x'}^2}\right) dx\, dx'$$

Fraction of particles enclosed within phase space ellipses

Phase space area	Fraction of particles enclosed in a Gaussian distribution	Fraction of particles enclosed in a top-hat distribution
$\pi\varepsilon_{x,rms}$	39%	25%
$4\pi\varepsilon_{x,rms}$	87%	100%
$6\pi\varepsilon_{x,rms}$	95%	

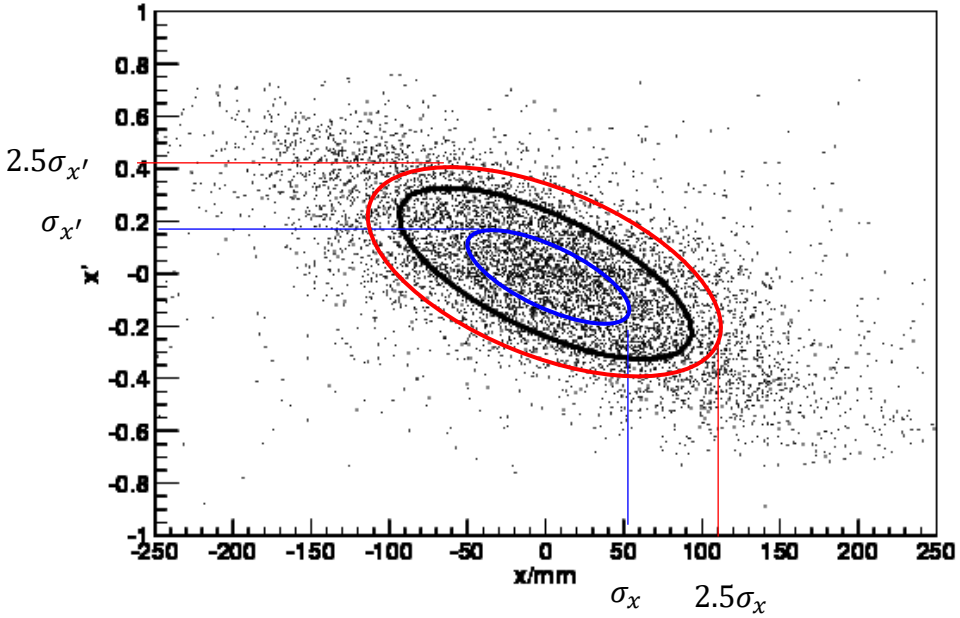

Phase-space area for Gaussian distributions in x and x'.
Blue = $\pi\varepsilon_{x,rms}$ **Black** = $4\pi\varepsilon_{x,rms}$ **Red** = $6\pi\varepsilon_{x,rms}$

For a top-hat (constant density) distribution, the rms radius is half of the maximum radius.

Emittance is in unit of mm-mrad (or μm).

Normalized Emittance & Brightness

x and z momenta at low energy

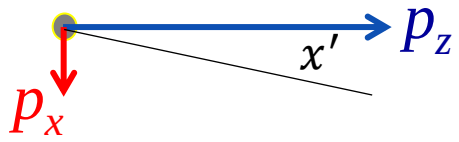

$$x' = \frac{p_x}{p_z}$$

x and z momenta at higher energy

Normalized emittance

$$\varepsilon^*_{x,rms} = \beta\gamma\varepsilon_{x,rms}$$

Normalized 95% phase-space area

$$\Sigma_x = 6\pi\varepsilon^*_{x,rms}$$

5D Beam brightness

$$B_{5D} = \frac{2I}{\pi^2\varepsilon^*_x\varepsilon^*_y}$$

$$B_{5D,95\%} = \frac{2I}{(6\pi)^2\varepsilon^*_{x,rms}\varepsilon^*_{y,rms}}$$

Sources of Emittance in RF Photoinjectors

$$\varepsilon_{total} = \sqrt{\varepsilon_T^2 + \varepsilon_{rf}^2 + \varepsilon_{SC}^2 + \varepsilon_B^2}$$

Intrinsic (thermal) emittance
Photocathode bandgap/work function
Laser photon energy
Photoemission radius

RF-induced emittance
RF wavenumber
Accelerating gradient
Beam radius
Bunch length
Electron phase at gun exit

Space charge emittance
Accelerating gradient
Beam energy
Peak current
Transverse & longitudinal current profiles
Emittance compensation with a solenoid

Angular momentum emittance
Magnetic field at the cathode
Photoemission radius

Mean Transverse Energy (MTE)

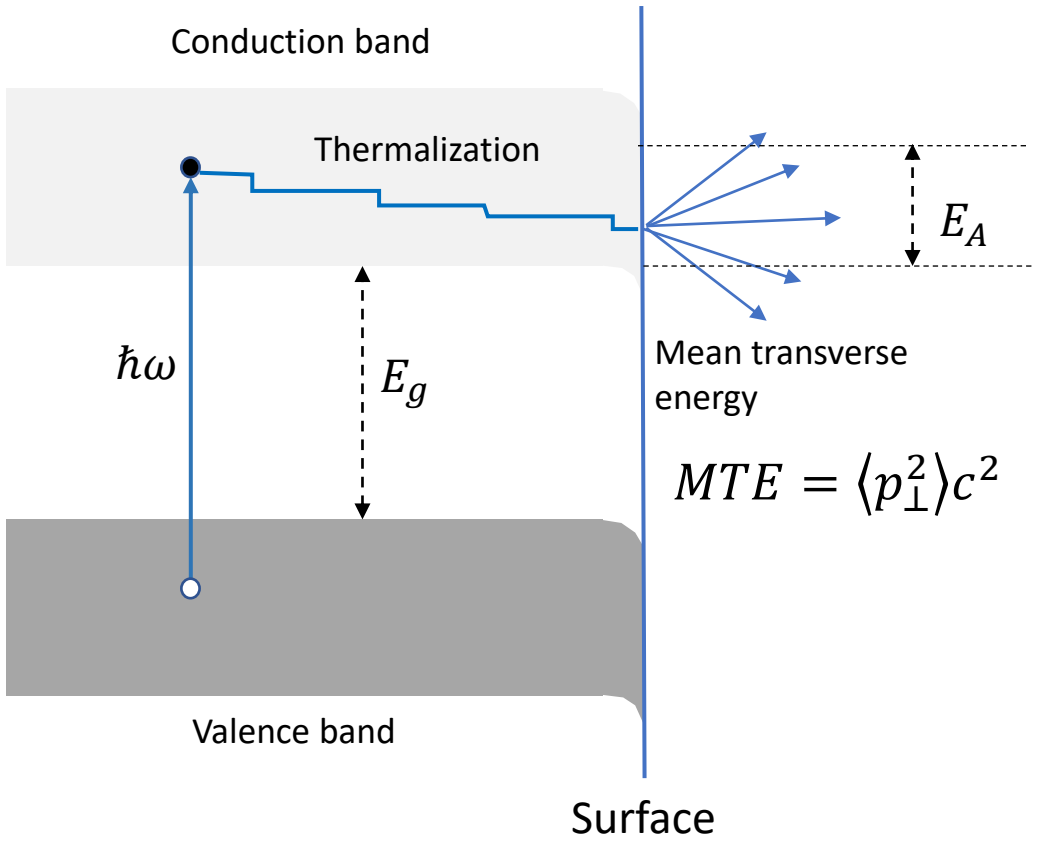

The normalized thermal emittance divided by photoemission radius depends on MTE which depends on the photocathode material, its surface roughness and the laser photon energy.

$$\varepsilon_{T,x} = \sigma_x \frac{\sqrt{\langle p_\perp^2 \rangle}}{m_e c} = \sigma_x \frac{\sqrt{MTE}}{m_e c^2}$$

Semiconductor photocathode

$$MTE \approx \frac{1}{3}\left(\hbar\omega - \left(E_g + E_A\right)\right)$$

Metal photocathode

$$MTE \approx \frac{1}{3}\left(\hbar\omega - \phi + \sqrt{\frac{\beta e E_0}{4\pi\epsilon_0}}\right)$$

Normalized Intrinsic (Thermal) Emittance

The normalized thermal emittance divided by the photoemission radius, in unit of μm/mm, is proportional to the square root of MTE.

$$\frac{\varepsilon_{T,x}}{\sigma_x} = \sqrt{\frac{MTE}{m_e c^2}}$$

	Cu	Mg	Cs_2Te	CsK_2Sb	Na_2KSb	Unit
$\hbar\omega$	4.9	4.7	4.7	2.3	2.3	eV
ϕ or $(E_g + E_A)$	4.4	3.6	3.9	2	2	eV
MTE	167	367	250	100	100	meV
$\frac{\varepsilon_{T,n}}{\sigma_x}$ calculated	0.4	0.8	0.7	0.44	0.44	μm/mm
min. measured	0.7	0.4	0.6	0.5		

Slice Emittance vs. Projected Emittance

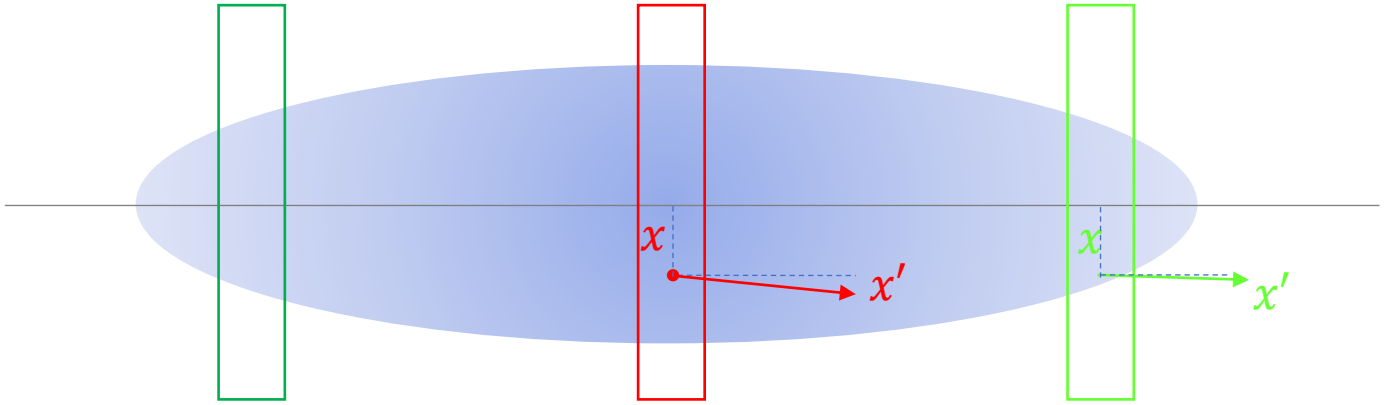

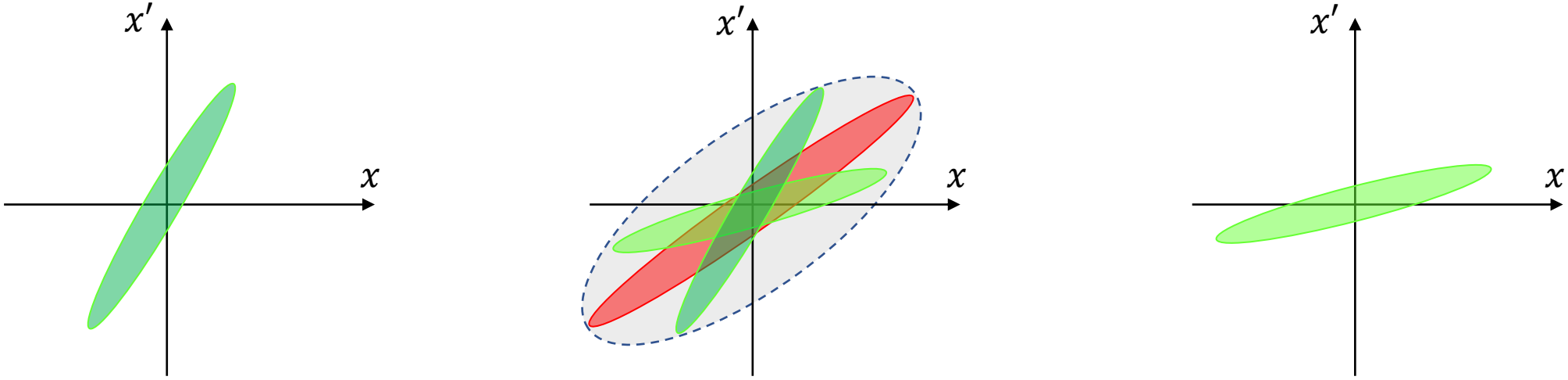

Different slices experience different RF kicks and space charge field, and therefore they have different phase space ellipses and orientations.

RF Induced Emittance

Different slices experience different RF focusing at the gun exit, depending on their radial size and exit phase.

$$x' = x\frac{eE_0}{2\beta\gamma m_e c^2} sin(\varphi_{exit})$$

Assuming the average exit phase of all particles is at the optimum phase of $\pi/2$, the RF induced emittance is given by

$$\varepsilon_{RF} = \frac{\alpha k^3 \sigma_x^2 \sigma_z^2}{\sqrt{2}}$$

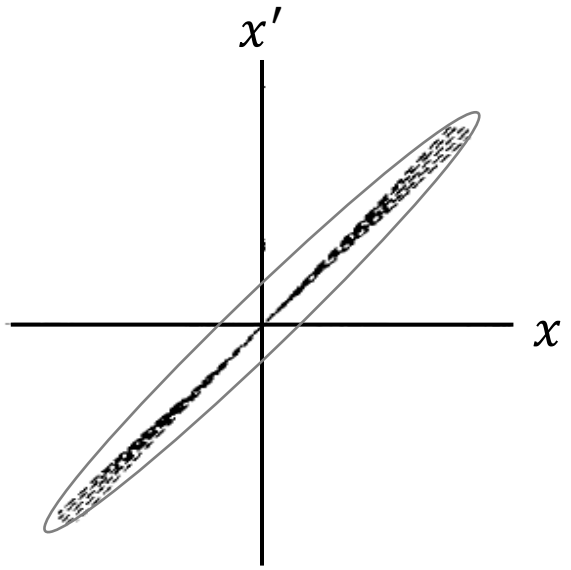

Individual slices with zero emittance fan out in phase space due to different RF focusing, resulting in finite RF induced emittance (ellipse).

Using a low-frequency gun (small k) will result in small RF-induced emittance. Recent RF photoinjector designs focus on low-frequency quarter-wave guns. Due to the DC-like nature of the accelerating field, these low-frequency QW photoinjectors have almost zero RF emittance.

Transverse Space Charge

Transverse SC force causes the beam to expand radially. Transverse force arises from charge density (radial electric field) and current density (azimuthal magnetic field).

$$\rho = \frac{I}{\pi R^2 v_z} \qquad J = \frac{Ir}{\pi R^2}$$

$$B_\theta = \frac{\mu_0}{2} Jr = \frac{v_z}{c^2} E_r$$

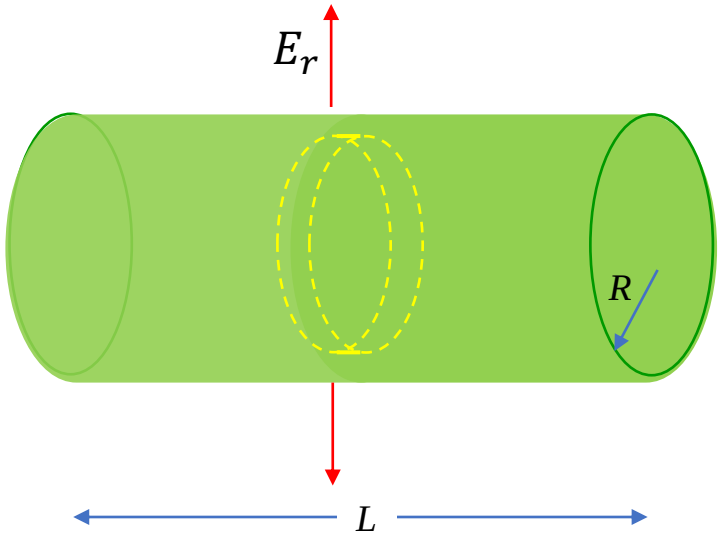

Transverse SC force scales with $1/\gamma^2$ and dominates at low energy

$$F_r = -e[E_r - v_z B_\theta] = -eE_r(1-\beta^2) = -\frac{eE_r}{\gamma^2}$$

$$E_r(r) = \frac{Ir}{2\pi\epsilon_0 R^2 \beta c} g(\zeta) \qquad \zeta = z - \bar{v}_z t$$

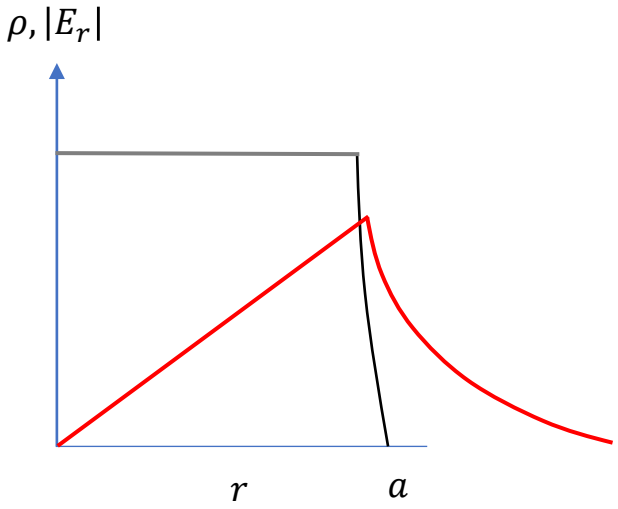

Space Charge Emittance Growth

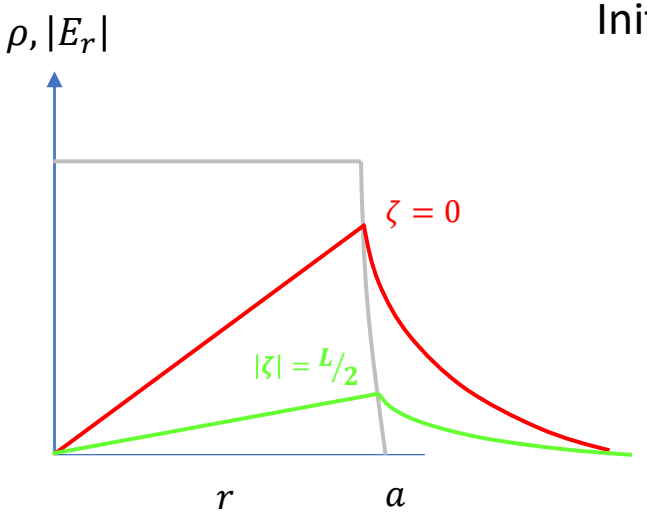

Initial phase spaces

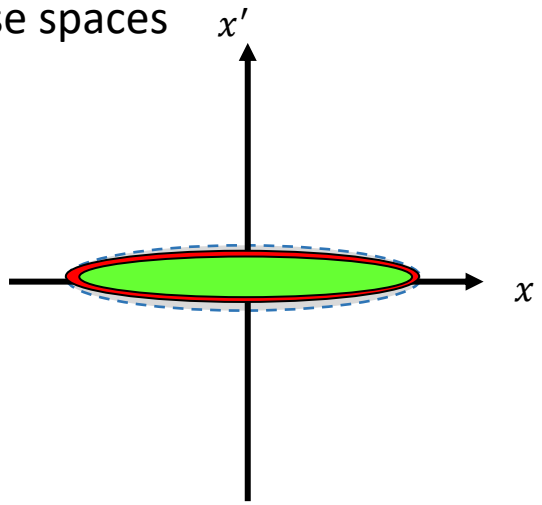

Phase-spaces after space charge

Projected emittance

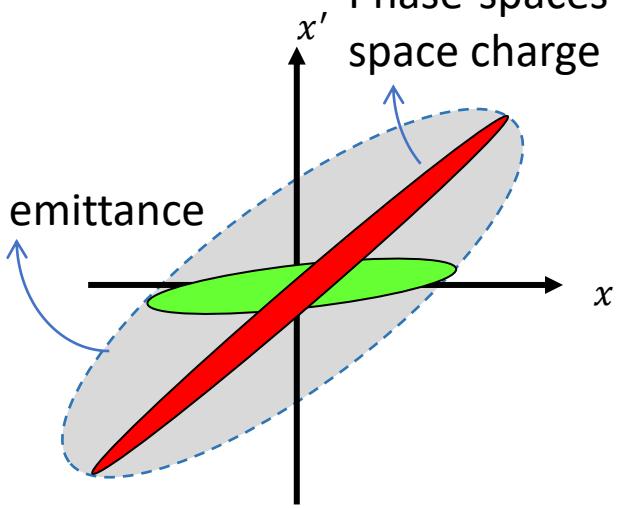

Radial SC electric field

$$E_r = -\frac{eE_r}{\gamma^2}$$

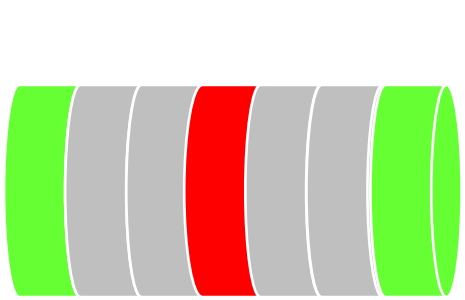

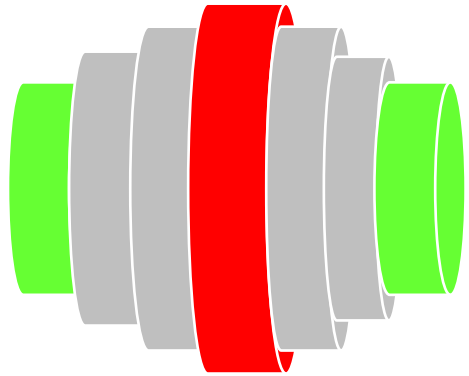

Electron bunch with N slices initially generated at cathode

Same bunch after drifting under space charge force

Space Charge Emittance for Gaussian Bunch

Define the aspect ratio for a Gaussian pulse $A = \frac{\sigma_x}{\sigma_z}$

Transverse and longitudinal SC form factors

$$\mu_x(A) = \frac{1}{3A + 5}$$

Space charge emittance for a Gaussian pulse

$$\varepsilon_{SC} = \frac{\pi}{4}\left(\frac{1}{\alpha k sin(\varphi_0)}\right)\frac{I}{I_A}\mu_x(A)$$

LCLS Cu S-band	Typical values
f	2,856 MHz
α	2
q	100 pC
σ_x	0.5 mm
σ_z	1.5 mm
I	10 A
ε_{SC}	0.7 mm-mrad

Space Charge Emittance for Uniform Cylinder

The aspect ratio for a uniform cylinder with radius a and length L

$$A = \frac{a}{L}$$

Transverse SC form factor

$$\mu_x(A) = \frac{1}{35\sqrt{A}}$$

Space charge emittance for a uniform cylinder

$$\varepsilon_{SC}(A) = \frac{\pi}{4}\left(\frac{1}{\alpha k sin(\varphi_0)}\right)\frac{I}{I_A}\mu_x(A)$$

LCLS Cu S-band	Typical values
f	2,856 MHz
α	2
q	100 pC
a	0.5 mm
L	3 mm
I	10 A
ε_{SC}	0.16 mm-mrad

Emittance Compensation

Carlsten (LANL) first introduced the idea of emittance compensation in 1989 after observing in simulations what appeared to be a violation of Liouville Theorem: the normalized emittance decreased as the electron beam traverses a solenoid magnet wrapped around the first photoinjector, which had only 0.5 cell. The original idea of using the solenoid was to focus the beam and counteract the RF defocusing effect of the radial RF field.

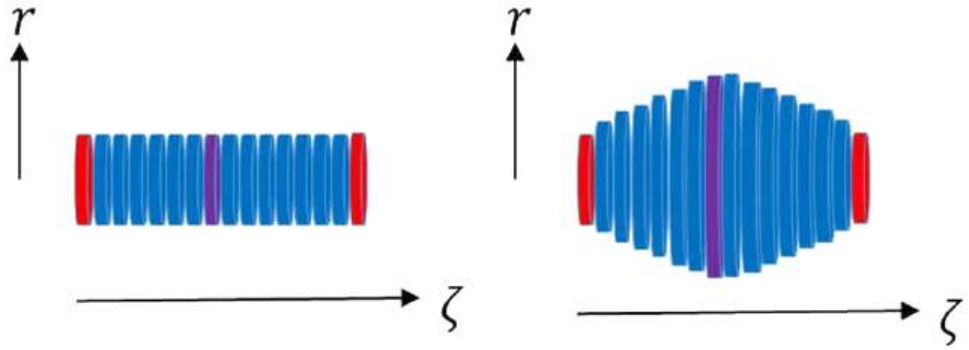

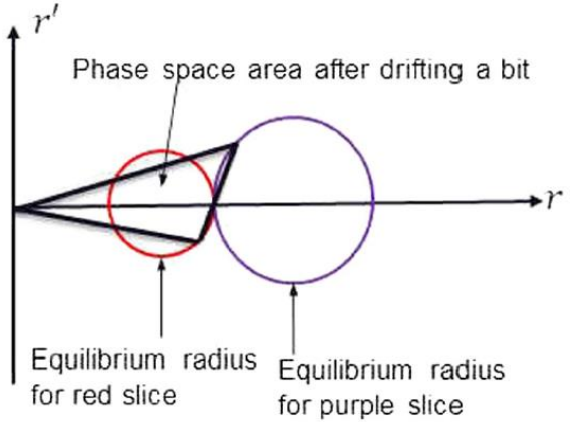

Carlsten's 1989 paper described emittance compensation as an alignment of different axial slices after they were inverted by the solenoid magnet, creating a smaller "projected" emittance. The reduced "projected" emittance was demonstrated experimentally at BNL by Qiu et al. in 1996.

B.E. Carlsten, Nucl. Instr. Meth. A 285, 313 (1989).
X. Qiu, K. Batchelor, I. Ben-Zvi, XJ Wang, Phys. Rev. Lett. 76, 3723 (1996).

Focusing with a Solenoid Magnet

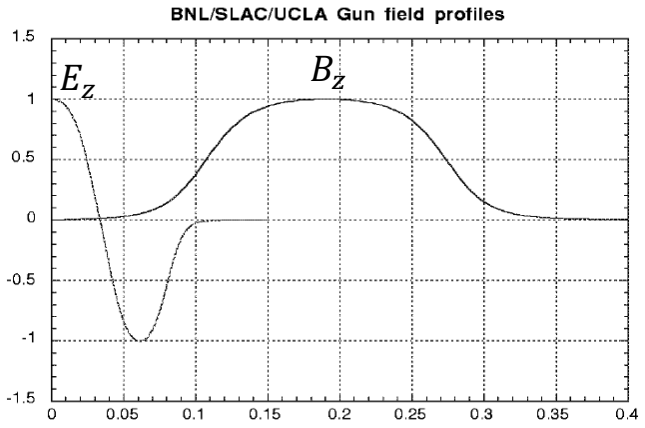

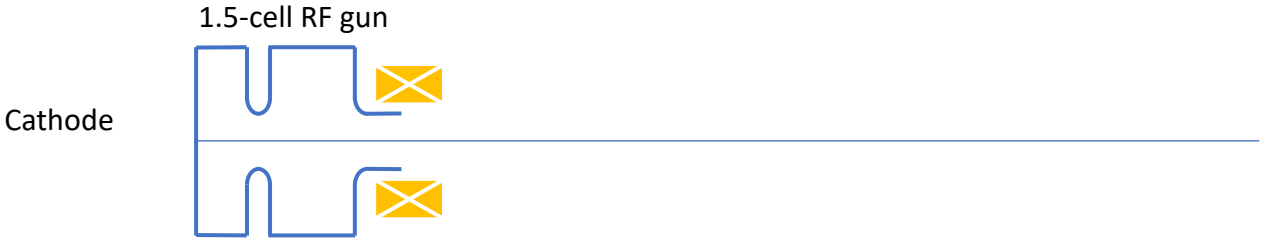

Canonical angular momentum

Paraxial ray equation

$$r'' + \left(\frac{eB_z}{2p_0c}\right)^2 r - \left(\frac{P_\theta}{p_0}\right)^2 \frac{1}{r^3}$$

Solenoid focusing

Repulsive centrifugal force

For the S-band gun with 1 mm emission radius, the CAM emittance is ~ 0.01 μm/Gauss of cathode magnetic field

rms radius (mm)

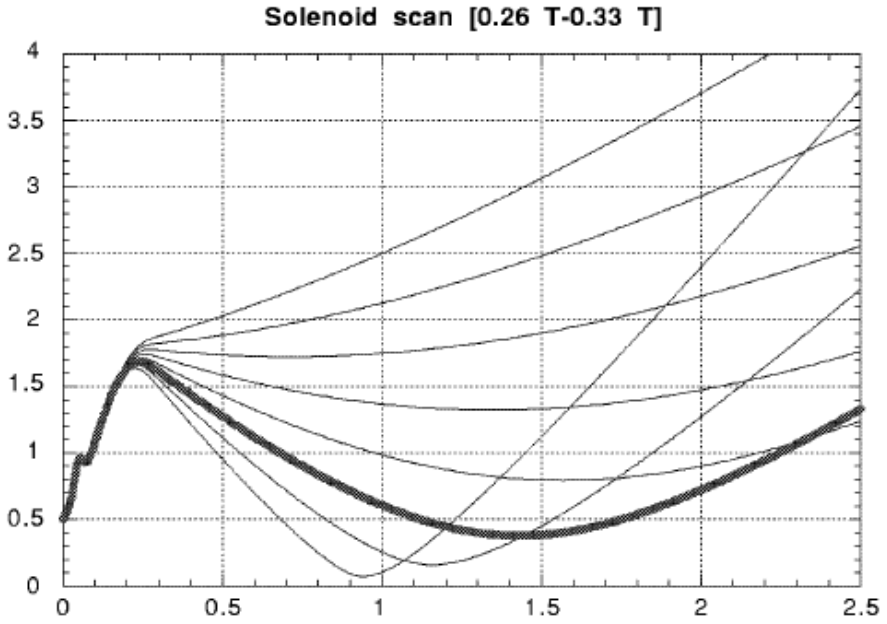

Courtesy of M. Ferrario

Emittance Oscillation & Invariant Envelope

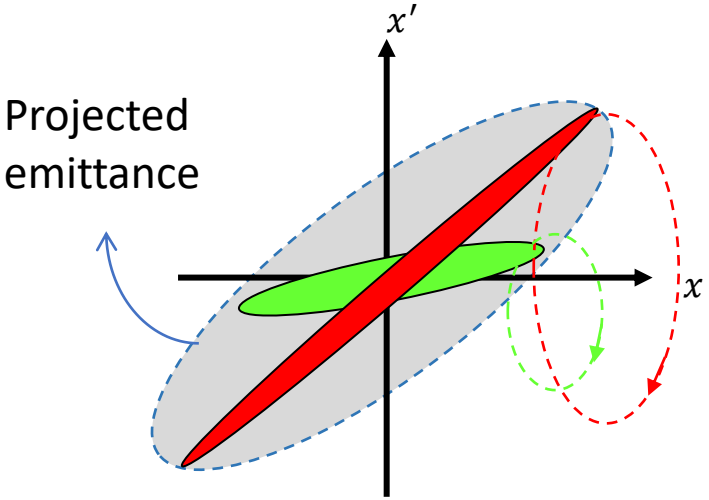

Transverse phase-space

Serafini and Rosenzweig analyzed the emittance oscillations based on plasma oscillations about the invariant envelope in 1997. Ferrario while at SLAC in 1998 developed the code HOMDYN to model the slice emittance and illustrate the emittance compensation clearly.

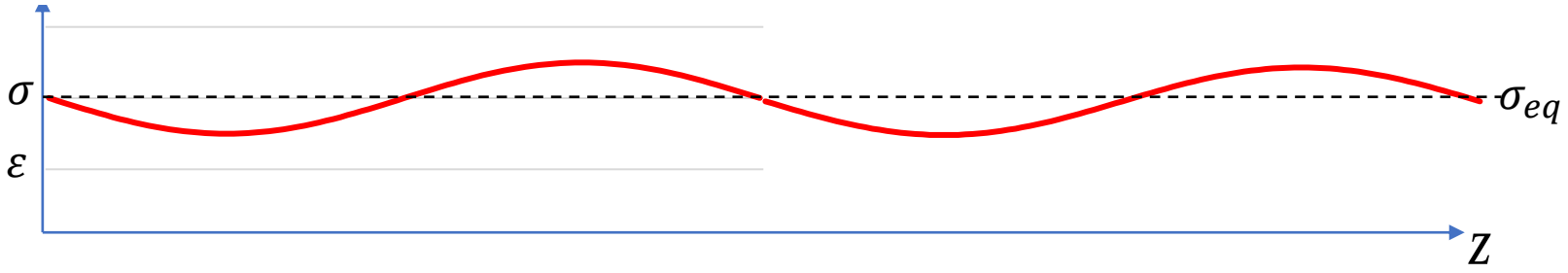

Solenoid wave-number

$$k_B = \frac{eB_0}{2\beta\gamma m_e c}$$

Envelope equation for zero-emittance beams

$$\sigma'' + k_B^2\sigma - \frac{K}{\sigma} = 0$$

Equilibrium envelope radius for space-charge dominated beams

$$\sigma_{eq} = \frac{\sqrt{K}}{k_B}$$

L. Serafini and J. Rosenzweig, Phys. Rev. E 55, pp. 7565-7590 (1997).
M. Ferrario et al., Technical Report No. SLAC-PUB-8400 (2000).

Paraxial Ray Equation including Space Charge

Paraxial ray equation for single particles in a constant solenoid field

$$r'' + k_B^2 r - \frac{\varepsilon_n^2}{r^3} - \frac{K}{a^2} r = 0$$

Focusing term due to solenoid magnetic field

Emittance pressure

Defocusing due to space charge

rms envelope equation

$$\sigma'' + k_B^2 \sigma - \frac{\varepsilon_n^2}{\sigma^3} - \frac{K}{\sigma} = 0$$

Emittance-dominated beams occur along the beamline where the beams have small radii

Reduced rms Envelope Equation

Reduced rms envelope

$$\hat{\sigma} = \sigma\sqrt{\gamma}$$

$$\hat{\sigma}'' + k_f^2\hat{\sigma} - \frac{\varepsilon_n^2}{\hat{\sigma}^3} - \frac{\kappa}{\gamma^2\hat{\sigma}} = 0$$

Focusing via solenoid and acceleration

$$k_f^2 = k_B^2 + \frac{3}{4}\left(\frac{\gamma'}{\gamma}\right)^2$$

Space-charge perveance

$$\kappa = K\gamma^3 = \frac{2I}{I_0}$$

Space charge to emittance ratio

$$\xi = \frac{\kappa\sigma^2}{\gamma\varepsilon_n^2}$$

Solutions to invariant envelope equation

Space-charge dominated, $\xi > 1$

$$\hat{\sigma}_{SC} = \frac{1}{\gamma'}\left(\frac{4\kappa}{3}\right)^{\frac{1}{2}}$$

$$\sigma_{SC} = \frac{2}{\gamma'}\left(\frac{I}{3\gamma I_0}\right)^{\frac{1}{2}}$$

Emittance-dominated, $\xi < 1$

$$\hat{\sigma}_{emit} = \left(\frac{2\gamma\varepsilon_n}{\sqrt{3}\gamma'}\right)^{\frac{1}{2}}$$

$$\sigma_{emit} = \left(\frac{2\varepsilon_n}{\sqrt{3}\gamma'}\right)^{\frac{1}{2}}$$

Emittance Compensation with a Short Solenoid

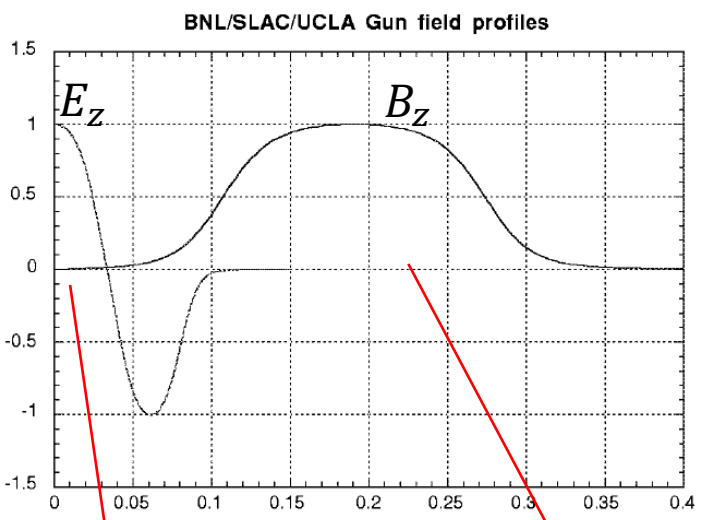

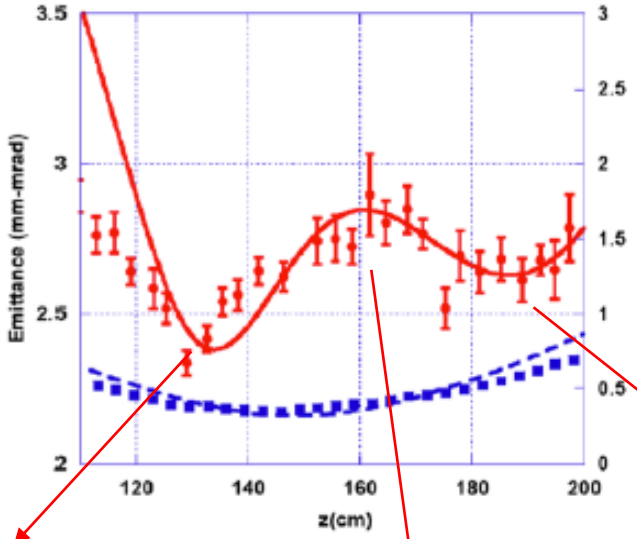

Courtesy of M. Ferrario

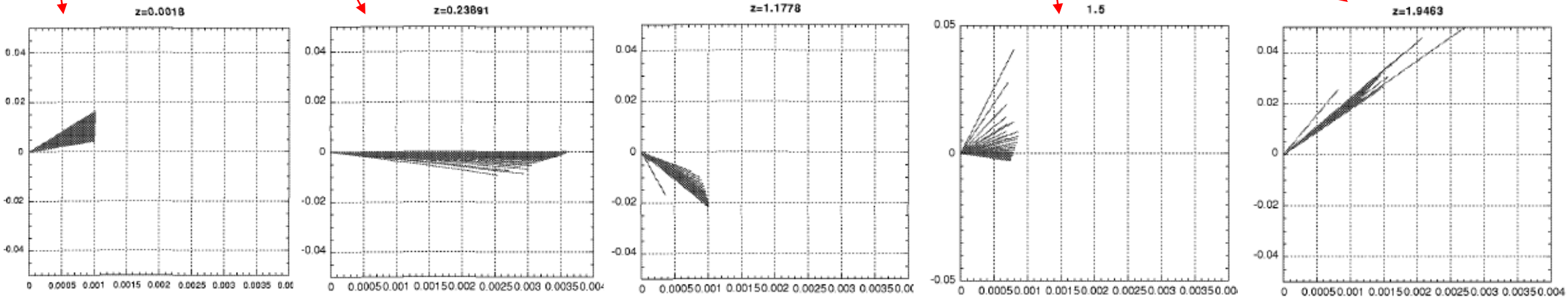

Transverse phase space at 5 different z (in m) as shown above the plots. The individual slices have zero emittance.

Damping Emittance Oscillations with a Booster

Booster entrance

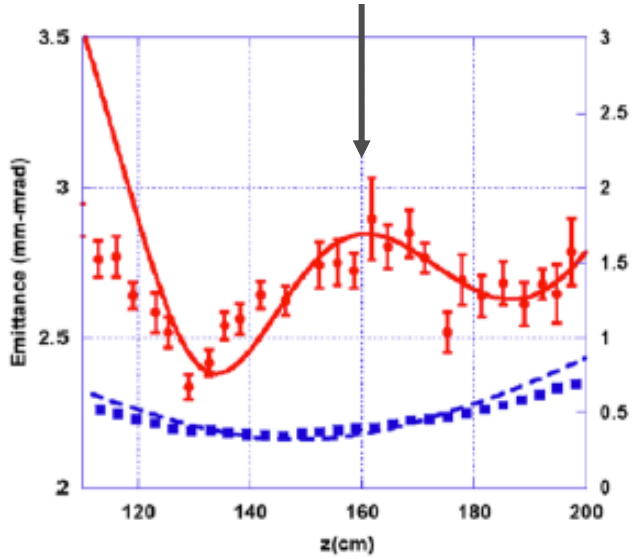

The beam is injected into the booster at the z location where the normalized emittance has a local maximum (between two minima). Acceleration in the booster linac damps the emittance oscillations at higher energy.

Plots of normalized emittance (blue) and rms beam radius vs z

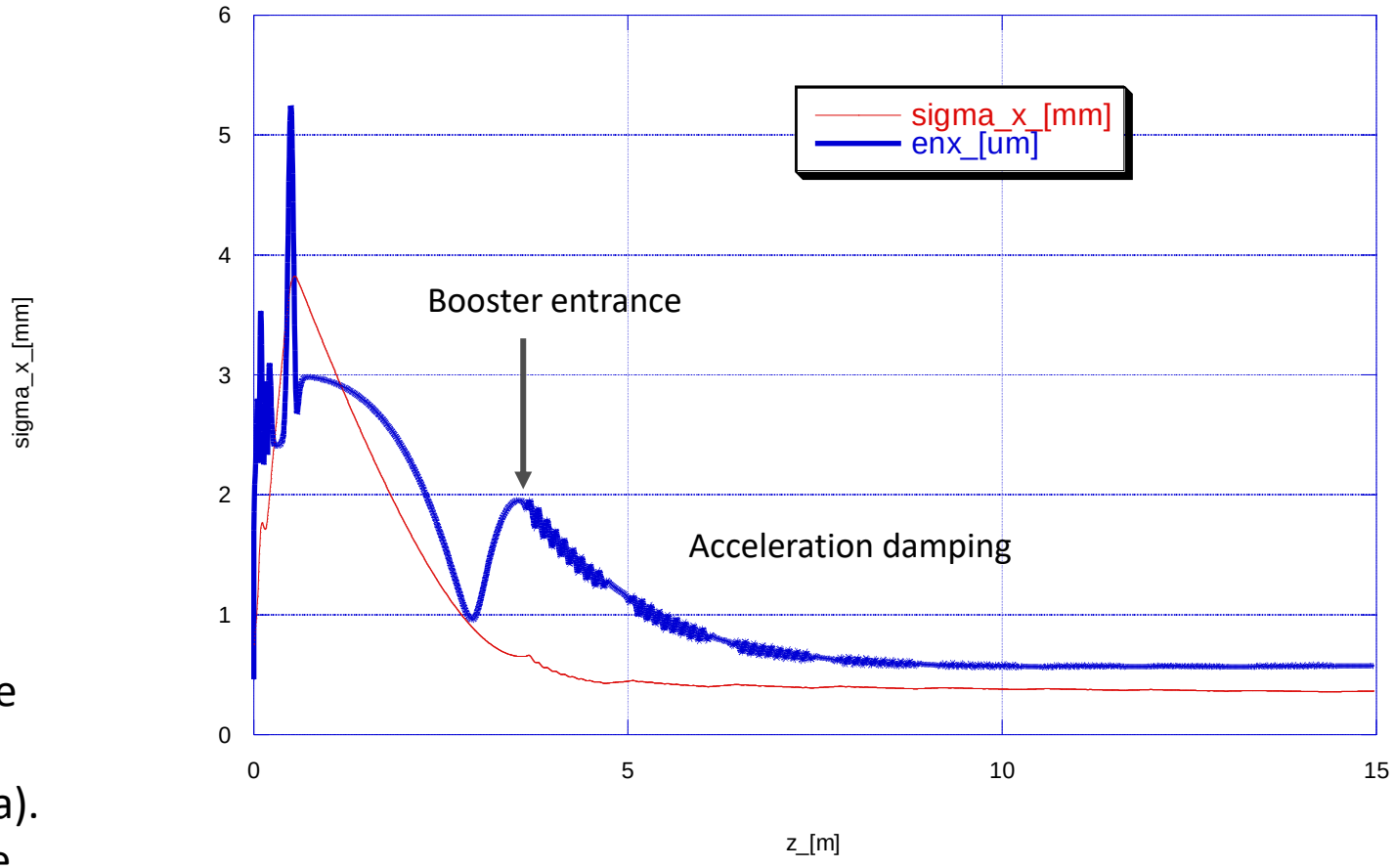

This optimum injection into the booster linac was introduced by Massimo Ferrario in 1998.

Courtesy of M. Ferrario

Emittance Minimization in RF Photoinjectors

Sources of Emittance		Minimization Approaches
• Intrinsic (thermal) emittance	⇒	• Use small laser beam radius • Select cathode/laser with low MTE
• RF induced emittance	⇒	• Use low-frequency resonators
• Space charge emittance	⇒	• Use high accelerating gradient at cathode • Use long laser pulses • Use solenoids to perform emittance compensation
• Emittance oscillations	⇒	• Match and accelerate beam in boosters properly
• Emittance due to B_{cathode}	⇒	• Null out magnetic field at the cathode

Photoinjector Designs

High-Frequency NCRF Gun (LCLS)

The 1.5-cell S-band electron gun is the work horse of the X-ray FEL at SLAC. Electrons are generated by ps UV pulses, 3rd harmonic of a Ti:Sap laser. At 100 pC, the electron beams have an rms normalized emittance at the undulator of 0.4 mm-mrad.

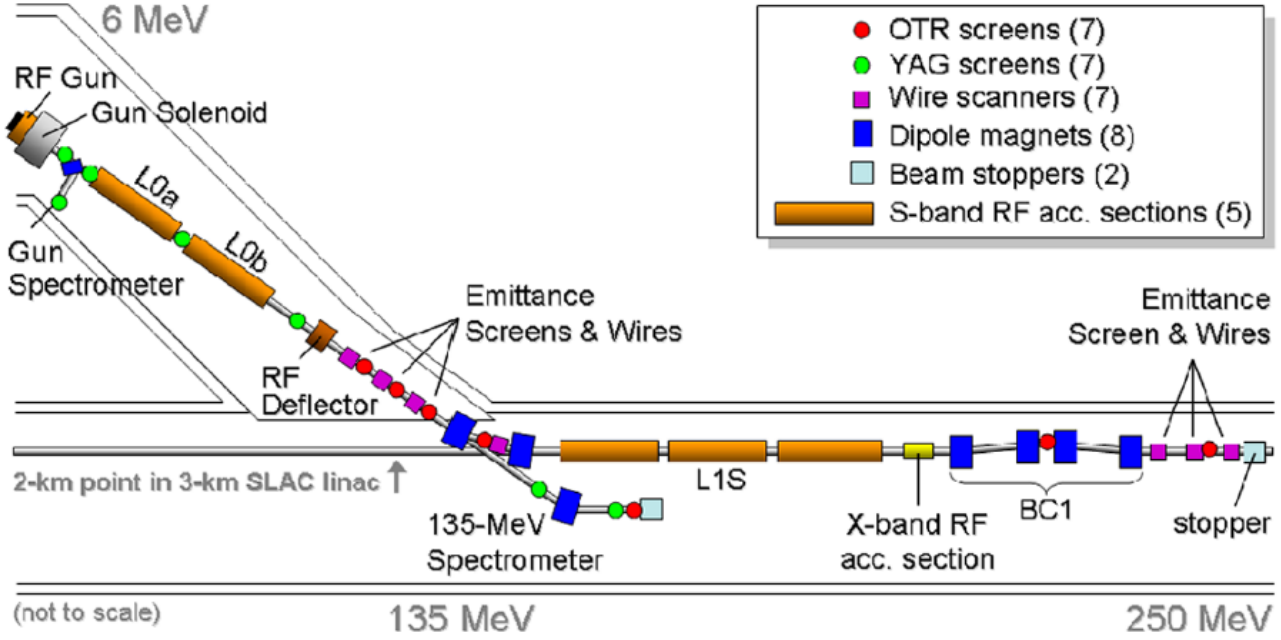

Cavity material	Copper
Cavity type	1.5-cell
Frequency	2,856 MHz
Temperature	30°C
Duty factor	0.012%
Cathode gradient	120 MV/m
Exit beam energy	6 MeV
Bunch charge	100 pC – 1 nC
Emittance @100pC	0.4 mm-mrad
Bunch rep rate	120 Hz
Photocathode	Copper

Low-Frequency NCRF Gun (Boeing)

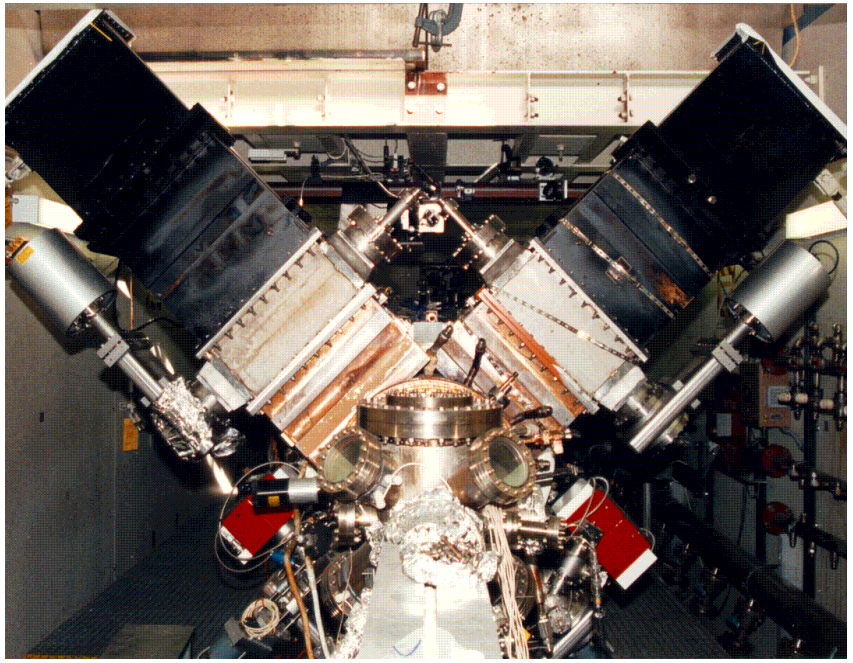

The Boeing 433-MHz electron gun still holds the record in average beam current (35 mA) for RF photoinjectors. The gun consists of 1.5 RF cells with re-entrant shapes and a solenoid coil imbedded in the wall between the two cells.

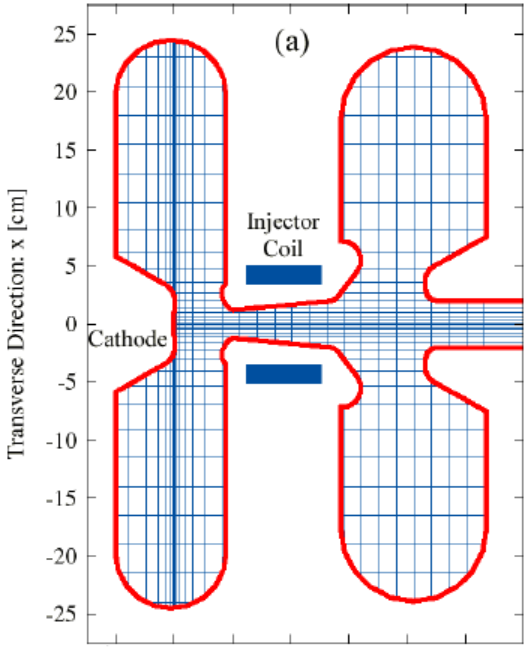

Cavity material	Copper
Cavity type	NC 1.5-cell
Frequency	433 MHz
Temperature	30°C
Duty factor	25%
Cathode gradient	20 MV/m
Exit beam energy	2 MeV
Bunch charge	1-7 nC
Emittance @4.5 nC	7 mm-mrad
Bunch rep rate	27 MHz
Photocathode	CsK_2Sb

Superconducting RF Gun (Rossendorf)

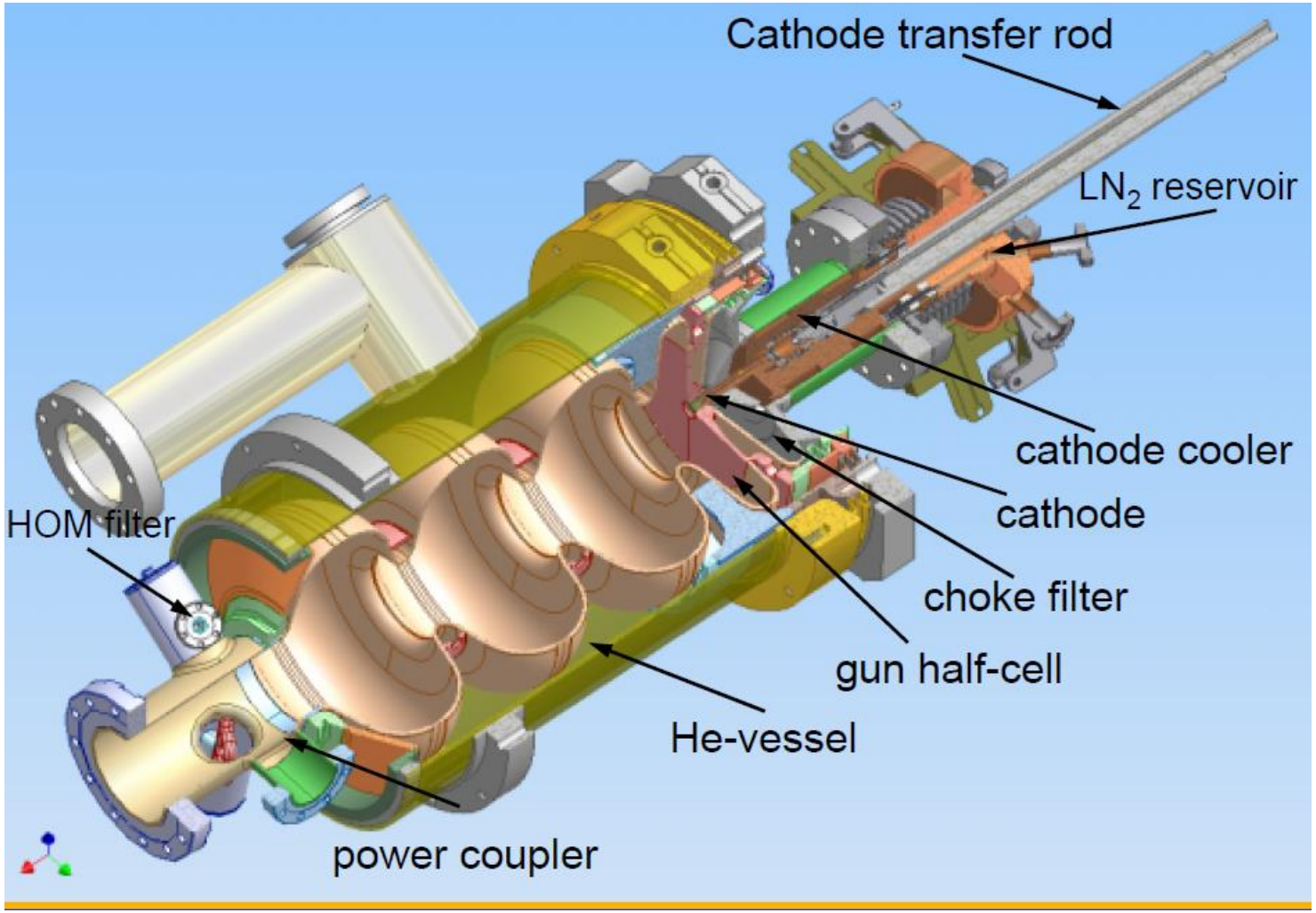

Cavity material	Niobium
Cavity type	SC 3.5-cell
Frequency	1,300 MHz
Temperature	1.9°K
Duty factor	CW
Cathode gradient	33 MV/m
Exit beam energy	9.5 MeV
Bunch charge	77 pC – 1 nC
Emittance @77pC	0.5 mm-mrad
Bunch rep rate	1 – 13 MHz
Photocathode	Cs_2Te

Coaxial Resonators

Half-wave resonator

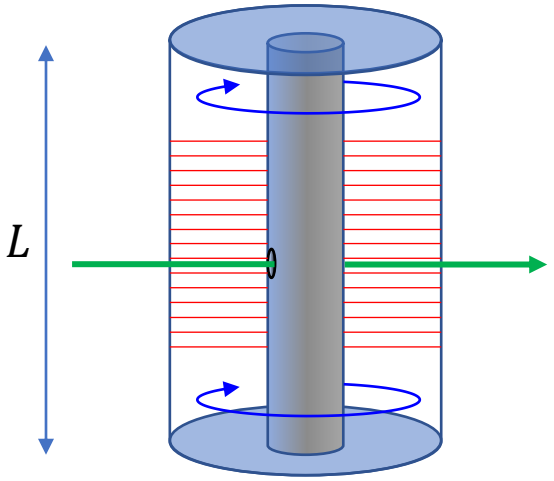

$$L = \frac{\lambda}{2}$$

Quarter-wave resonator

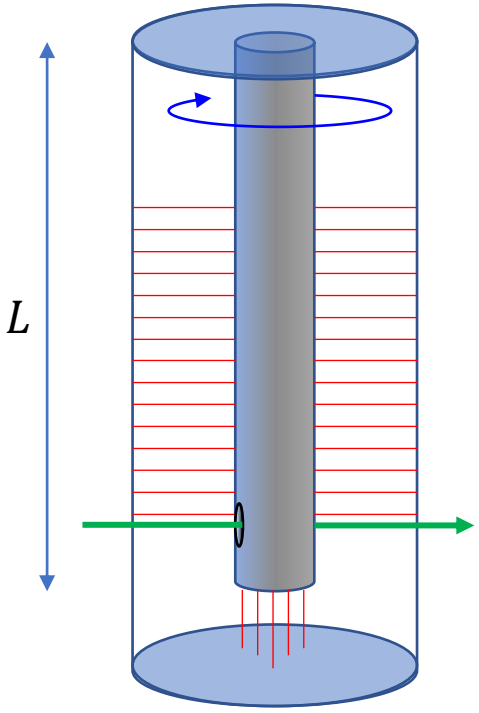

$$L = \frac{\lambda}{4}$$

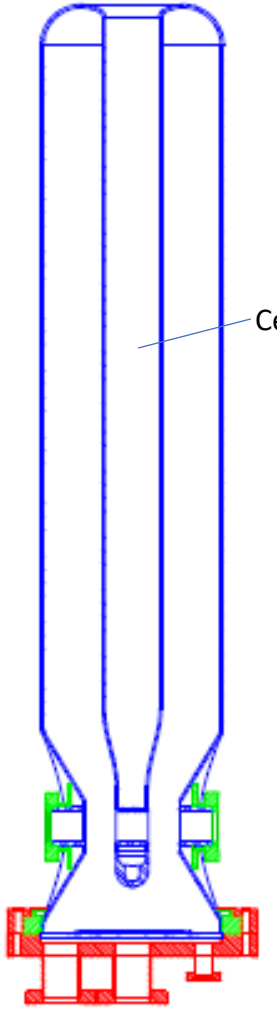

Rotated quarter-wave resonator
QWR photocathode gun

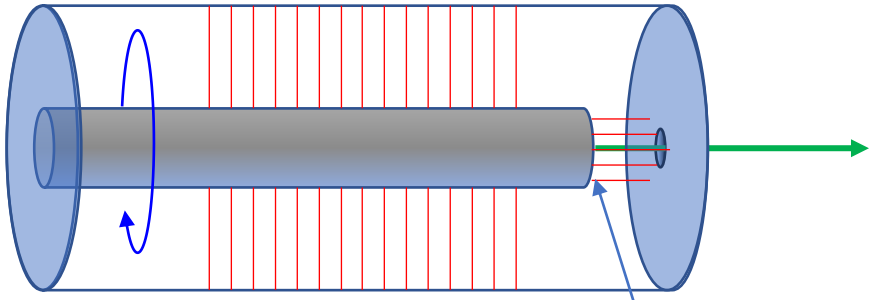

Low-Frequency Quarter-Wave Resonator Gun

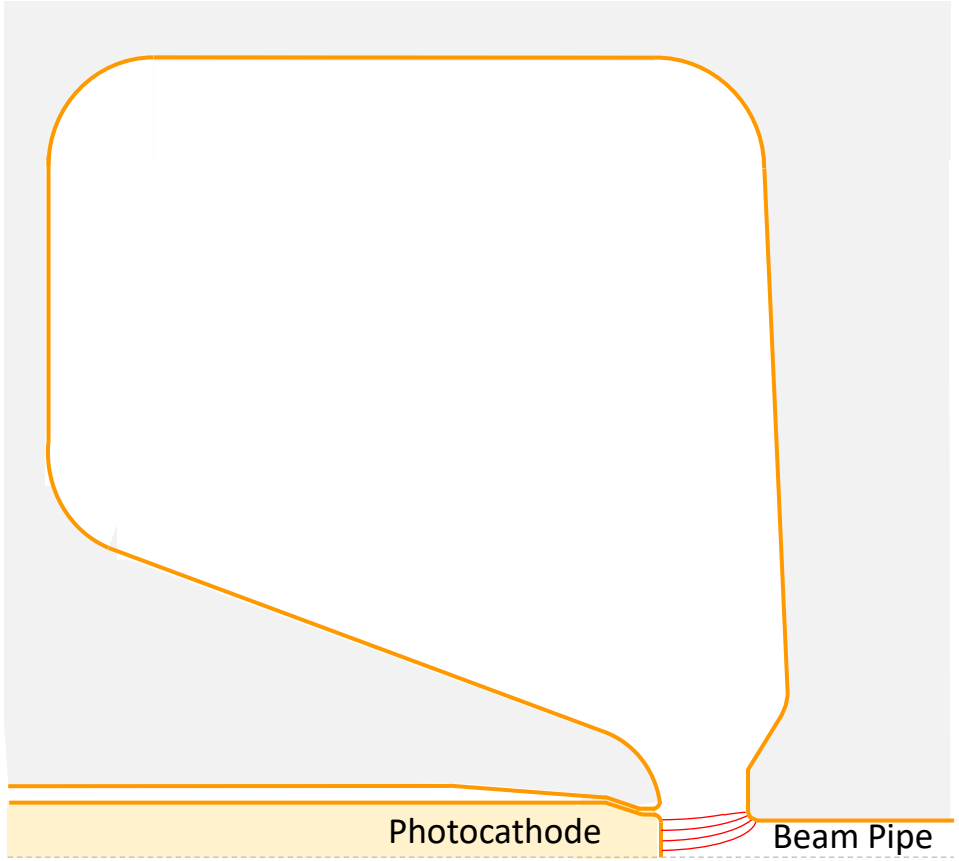

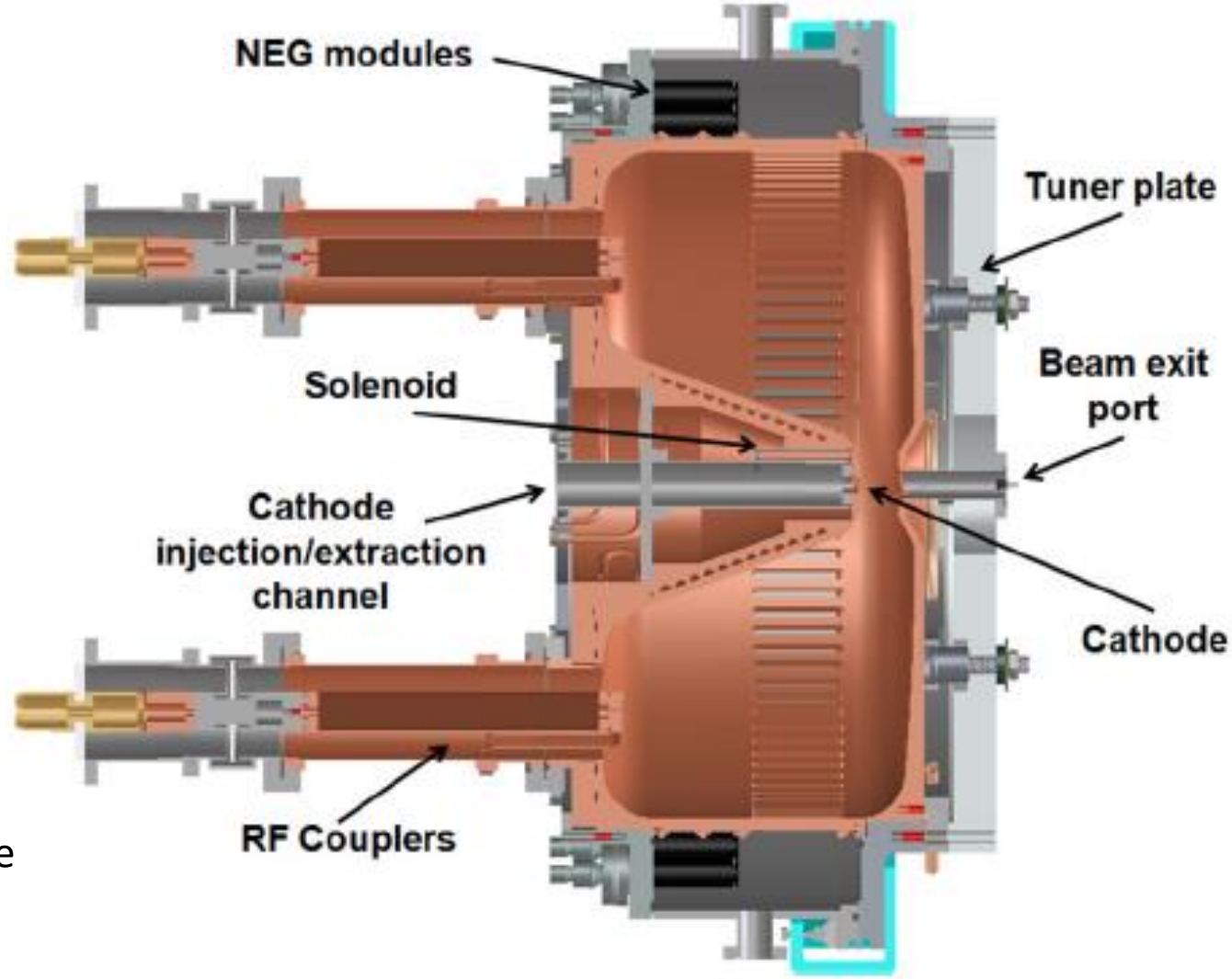

The electric field in a low-frequency QWR behaves like a DC field. The radial component of the electric field causes the beam to be defocused at the gun exit.

LCLS-II Gun & Buncher

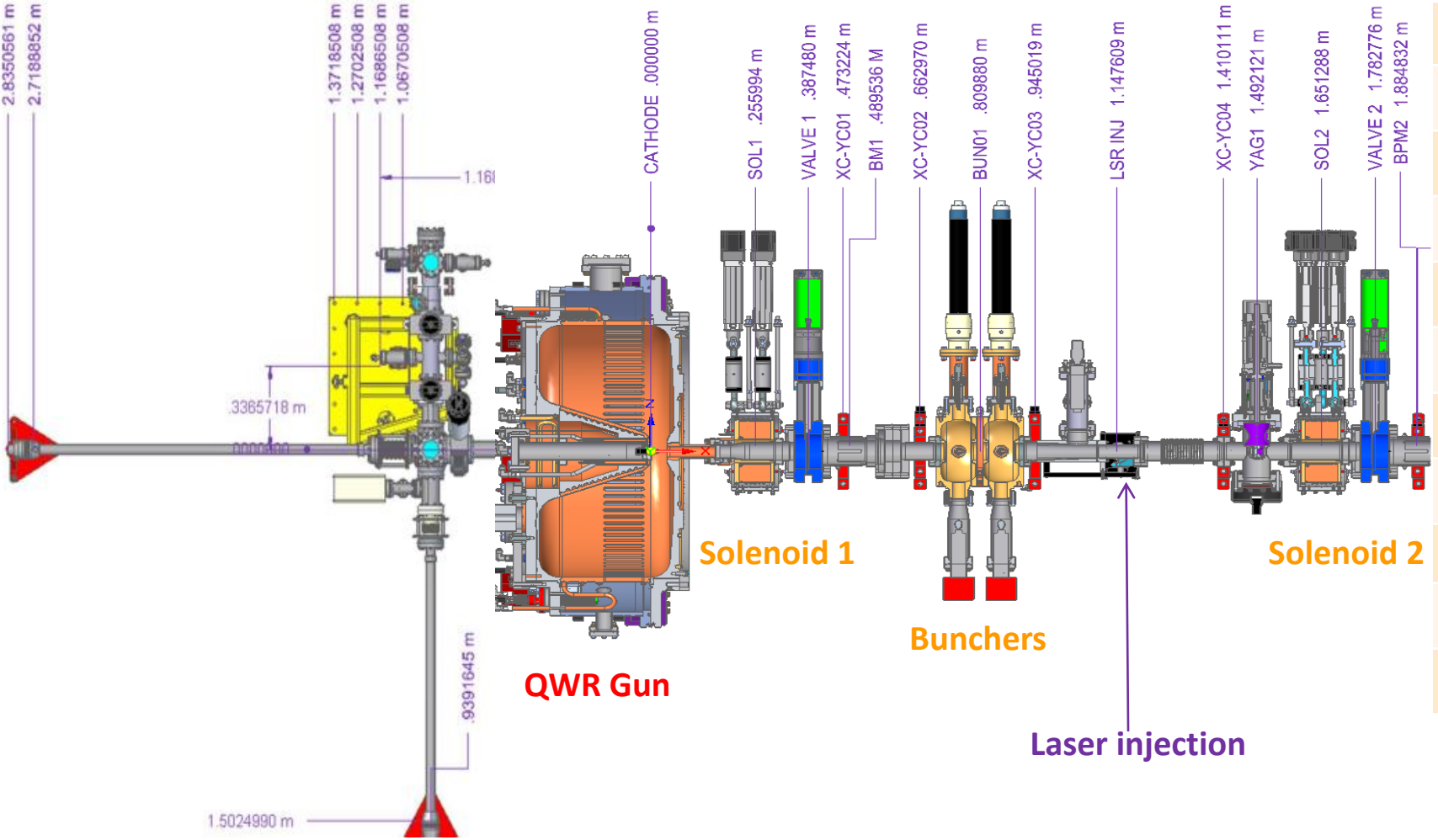

Cavity material	Copper
Cavity type	NC QWR
Frequency	185.714 MHz
Temperature	30°C
Duty factor	CW
Cathode gradient	20 MV/m
Exit beam energy	750 kV
Bunch charge	100 pC
Emittance @100pC	0.4 μm (Gaussian)
Bunch rep rate	928.57 kHz
Photocathode	Cu, Cs_2Te

Low-Frequency Superconducting QWR Gun

The low-frequency QWR design operates in a pseudo-DC mode with nearly constant field when the electron bunch is between the gap, thus minimizing RF-induced emittance.

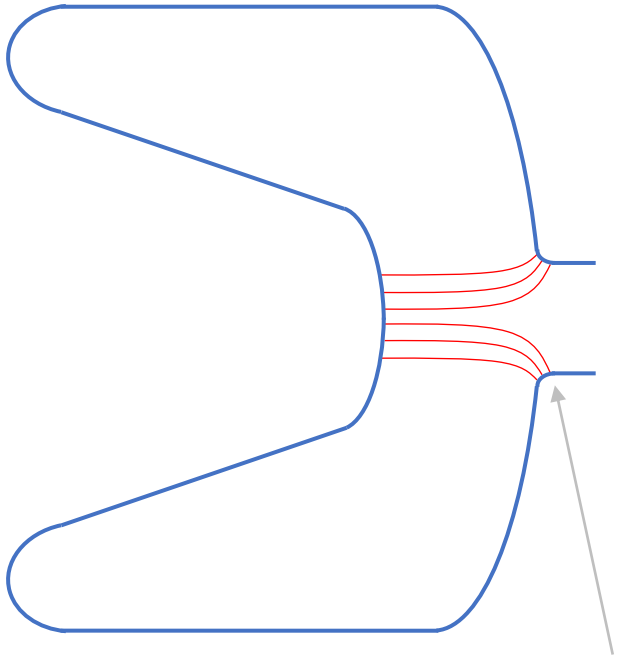

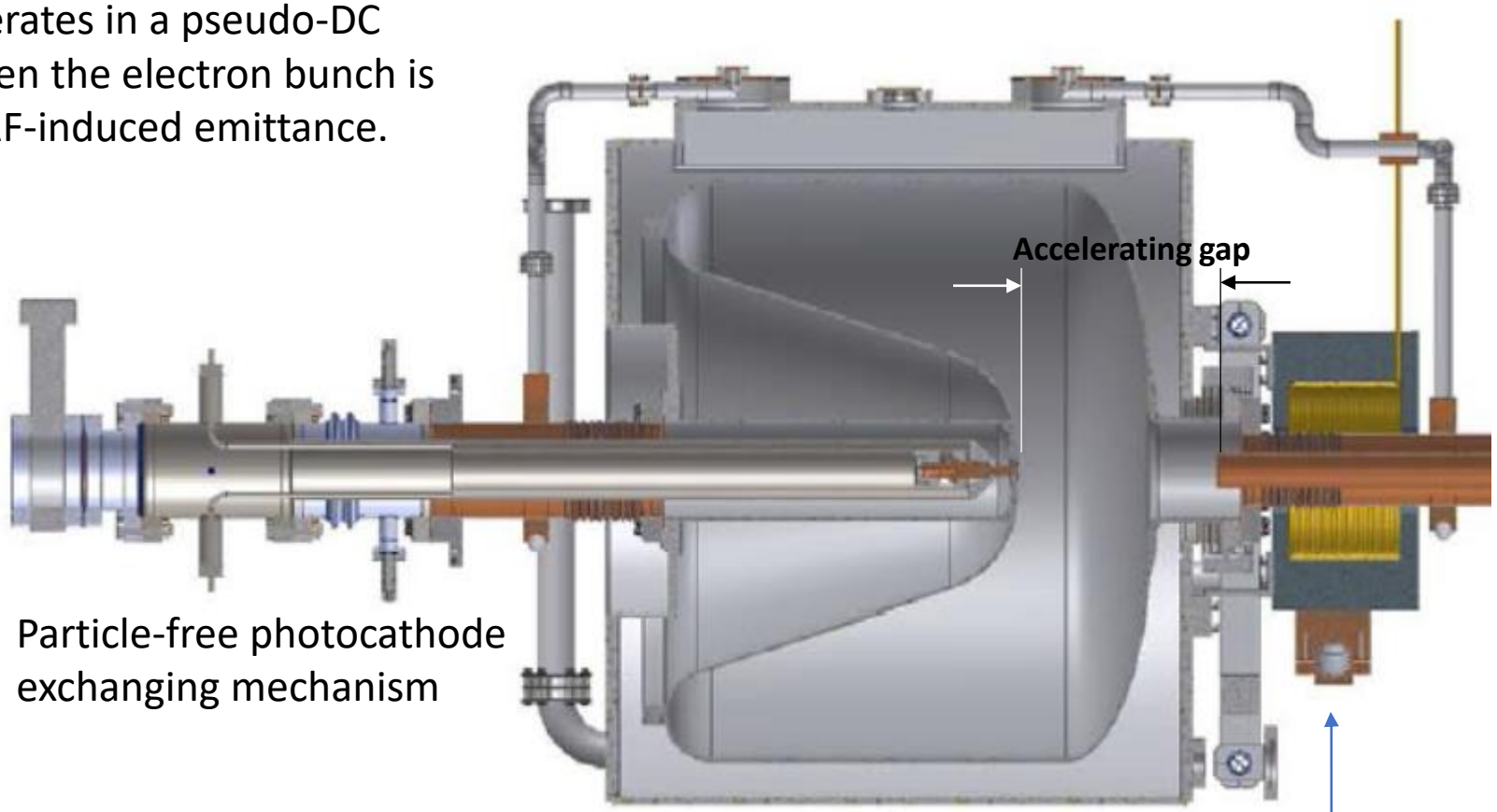

Particle-free photocathode exchanging mechanism

Field curvature near the gun exit causes radial defocusing that has to be corrected with a high-Tc superconducting solenoid.

Low-Frequency SC QWR Gun (WiFEL)

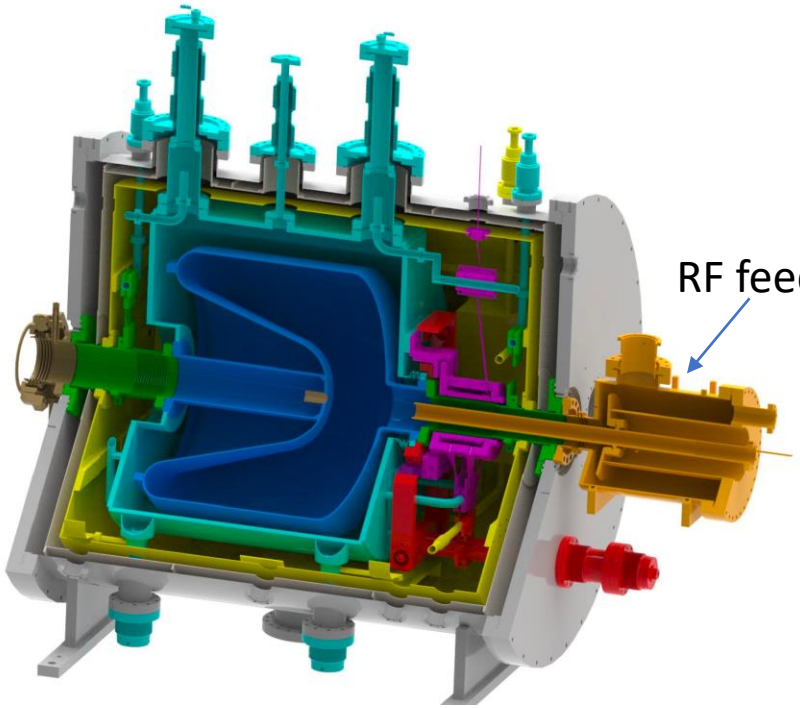

The hollow coaxial conductor acts like a dark current filter

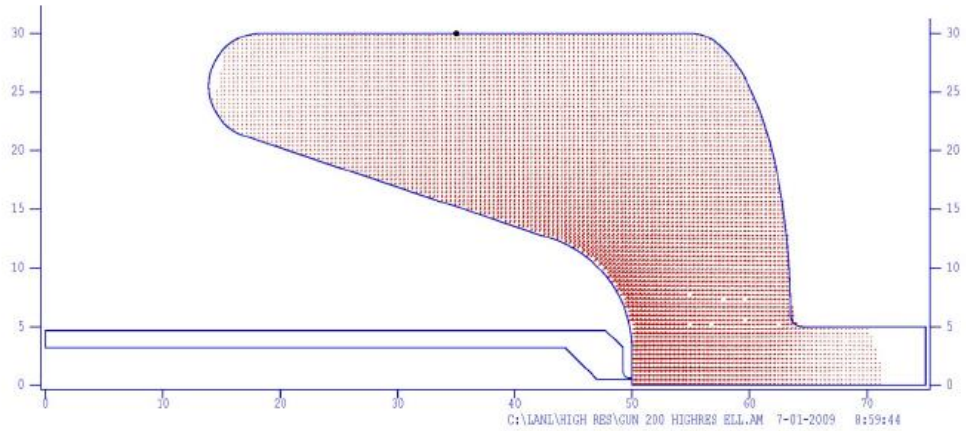

Dark current around the cathode ring

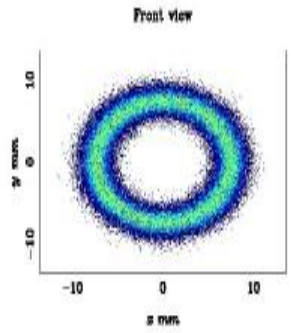

Cavity material	Niobium
Cavity type	SC QWR
Frequency	199.6 MHz
Temperature	4.2°K
Duty factor	CW
Cathode gradient	20 MV/m
Exit beam energy	4.5 MeV
Bunch charge	77 pC
Emittance @77pC	0.85 mm-mrad
Bunch rep rate	Up to 5 MHz
Photocathode	Cs_2Te

Reshaping the Cavity Shape of SC QWR Gun

Pipe radius = 5 cm (original)

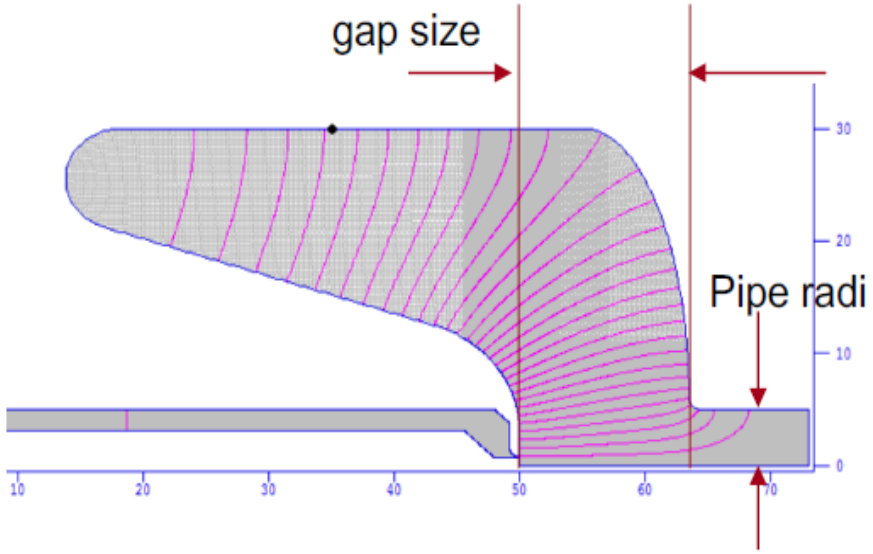

Accelerating gap = 13.5 cm

Beam pipe radius = 5 cm

RF wavelength = 150 cm

Pipe radius = 2 cm

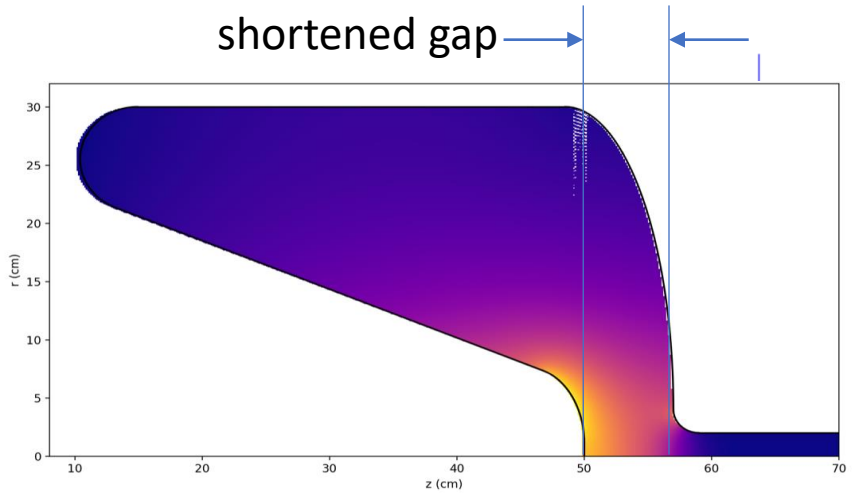

Accelerating gap = 7 cm

Beam pipe radius = 2 cm

RF wavelength = 161 cm

Photoinjector Simulation Codes

RF and Magnet Design Codes: These codes model the gun cavities via time and frequency domain solvers, as well as designing the solenoid magnets.

- SUPERFISH-POISSON: free codes from LANL; 2D
- MicroWave Studio: commercial code from CST; 3D

Particle Tracking Codes: These codes integrate the macroparticle trajectories under Lorentz forces, including space charge.

- IMPACT-t: particle tracking code from LBNL
- OPAL: free parallel code from PSI
- GPT: Commercial code from Pulsar Physics
- PARMELA: free code from LANL (also commercially available as T-STEP)

Accelerator Codes:

- elegant: free code from ANL
- B-MAD
- IMPACT-z

Summary

- Photoinjectors produce picosecond bunches of electrons with sufficiently high bunch charge and low transverse emittance as the first step in the generation of high-brightness electron beams for driving modern X-ray FELs.
- Emittance is an important property of electron beams as it determines the shortest wavelength that can be produced in an X-ray FEL.
- Quarter-wave resonators operate in the continuous-wave, DC-like mode to mitigate RF-induced emittance growth and support high-rep-rate operation.
- Superconducting QWR photoinjectors could produce the high-average-current, low-emittance electron beams needed to drive the next-generation X-ray FELs.